Irreversible Electroporation Applications

Brittanie Partridge, Melvin F. Lorenzo, Nikolaos Dervisis, Rafael V. Davalos, and John H. Rossmeisl

Abstract

In veterinary medicine, irreversible electroporation (IRE) applications have been evaluated in several early phase clinical trials evaluating the safety and feasibility of treatment of solid tumors located within different organ systems. These clinical trials support the use of IRE as a safe and effective alternative treatment option for tumors that are otherwise not amenable to current standard of care therapy. The recent development of high-frequency irreversible electroporation (H-FIRE) has made treatment delivery even more feasible for veterinary clinical patients. Here, we provide an overview of treatment planning and techniques while acknowledging current limitations associated with treatment delivery, followed by a review of IRE applications in veterinary clinical trials of spontaneous cancers. Lastly, we review the application of IRE in preclinical normal animal models or experimentally induced tumors as results of these studies may help facilitate translation of IRE into standard clinical practice.

B. Partridge · J. H. Rossmeisl (✉)
Veterinary and Comparative Neuro-oncology Laboratory, Department of Small Animal Clinical Sciences, Virginia-Maryland College of Veterinary Medicine, Virginia Tech, Blacksburg, VA, USA
e-mail: jrossmei@vt.edu

M. F. Lorenzo · R. V. Davalos
Virginia Tech – Wake Forest University, School of Biomedical Engineering and Mechanics, Virginia Tech, Blacksburg, VA, USA

N. Dervisis
Department of Small Animal Clinical Sciences, Virginia-Maryland College of Veterinary Medicine, Blacksburg, VA, USA

J. A. Impellizeri (ed.), *Electroporation in Veterinary Oncology Practice*,
https://doi.org/10.1007/978-3-030-80668-2_7

Keywords

IRE applications · H-FIRE · Animal models · Tumor ablation · Liver tumors · Brain tumors · Prostate cancer · Pancreatic cancer · Mammary cancer

1 Irreversible Electroporation Theory and Techniques

Irreversible electroporation (IRE) is an attractive nonthermal ablation method that uses high voltage (500–3000 V) pulsed electric fields (PEFs) of short duration (100 μs) to increase the transmembrane potential of cells and cause cell membrane disruption (Fig. 1a and Table 1). In response to a high-voltage PEF, the cell membrane forms electrically conducting nanopores to stabilize the transmembrane potential (Weaver and Chizmadzhev 1996). As the transmembrane potential is proportional to the locally applied electric field, the PEF protocol dictates whether the electroporation effects are transient or will lead to irrevocable damage. Under certain pulsing protocols, this process is reversible and has historically been applied in this manner to introduce genes and drugs into cells that would normally be impermeant to the cell membrane. However, once the applied electric field exceeds the threshold required to induce irreversible electroporation, the exposed cells will undergo cell death (Rubinsky 2007; Arena et al. 2011a; DeBruin and Krassowska 1999). As the electric fields which induce electroporation follow a sharp sigmoidal response, tissue ablation with IRE resolves within a submillimeter demarcation between treated and nontreated tissues (Potocnik et al. 2019). A major advantage of IRE compared to other ablation methods is that treatment results in minimal thermal damage due to negligible Joule heating of treated tissue, except for that lying immediately adjacent (<~1 mm) to the electrode edges where the electric field is greatest (Arena et al. 2011a). Contrary to thermal ablation methods, IRE is not prone to the phenomenon known as the "heat sink effect," in which larger blood vessels act to dissipate heat from surrounding tissue by means of conduction and convection heat transfer (Ahmed et al. 2011). Rather, cell death occurs at nearly discrete electric field thresholds and thus, treatment volumes are predictable and represented by a well-defined ablation zone following IRE delivery (Edd and Davalos 2007). Thus, its nonthermal cell death mechanism allows for treatment in otherwise inoperable locations, such as near major blood vessels and nerves. Taken together, the clinical advantages afforded from IRE therapy have resulted in improved overall survival in patients with pancreatic cancer (Kwon et al. 2014; Martin et al. 2013; Narayanan et al. 2012; Scheffer et al. 2014a, b). The promising early responses have led to the Food and Drug Administration granting an Expedited Access Pathway (EAP) designation to the IRE-based NanoKnife System to commercialize this therapy for widespread use.

IRE has demonstrated high efficacy for treatment of unresectable tumors, though improvements have recently been identified and engineered. Traditional IRE uses monophasic/unipolar pulses characterized by low frequency components; it is known that low frequency electric currents preliminarily traverse the extracellular

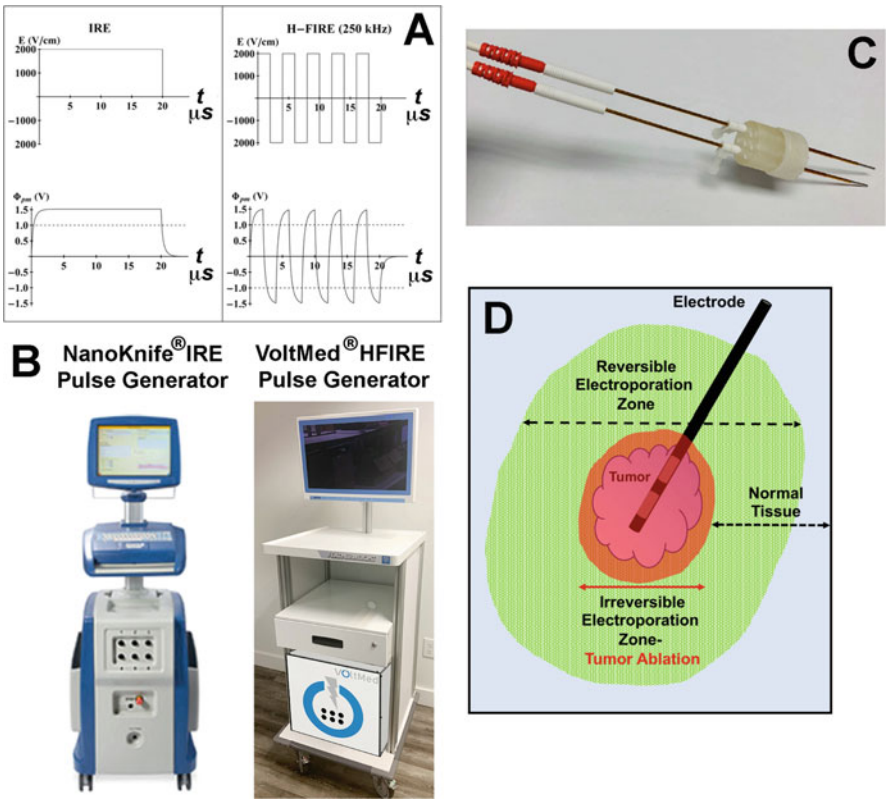

Fig. 1 (**a**) Comparison between IRE (left) and H-FIRE (right) pulses. IRE employs monopolar pulses of <100μs duration. H-FIRE pulse cycles consist of a series of ultrashort 0.5–2μs pulses of alternating polarity separated by 0.5–5μs of no energy delivery. Cycles are repeatedly delivered (10–100 cycles) to form bursts which are delivered at a ~1 Hz frequency. Amplitude of voltage delivery ranges from 0.25 to 5.0 kV. (**b**) NanoKnife IRE and INSPIRE H-FIRE pulse generators. (**c**) Blunt-tipped monopolar H-FIRE electrodes for use in the brain. (**d**) Schematic representation of electroporation treatment paradigm. Electrodes are inserted into the target tissue and used to deliver pulses that expose target tissue to the critical electrical field threshold that results in irreversible electroporation and tumor ablation (red). Cells further away from the electrodes and exposed to a smaller electrical field will undergo reversible electroporation

domain prior to cell electroporation. Thus, IRE pulses may be more susceptible to large impedance changes due to electroporation and may become disrupted by the impedance barrier of poorly conductive epithelial layers, including the skin (Bhonsle et al. 2015). High-frequency irreversible electroporation (H-FIRE) is a next generation IRE method that uses bursts of ultrashort (<10 μs) bipolar (Fig. 1a) PEFs to selectively ablate cells within a target volume (Arena et al. 2011b). As the characteristic frequencies associated with ultrashort PEFs (biphasic 1 μs pulses = 500 kHz) are higher than that of IRE (pulsed DC), H-FIRE is less susceptible to field distortions caused by heterogenous tissues and can overcome the impedance barrier

Table 1 Summary of treatment-related characteristics unique to ECT, IRE, and H-FIRE

Method	Pulse parameters	Treatment planning/ delivery	Limitations
ECT	Electric field threshold: <1000 V/cm Pulse duration: 50–100μs Pulse polarity: unipolar/ monophasic Pulse delivery rate: 1 Hz or 5 kHz	Flat plate electrodes[a,b] Linear array of needle electrodes Hexagonal array of needle electrodes Finger electrodes: axial or perpendicular needle electrodes At least 2 monopolar probes placed parallel to each other Neuroparalytic/muscle relaxant: local anesthetic administered	Requires multiple probes to be precisely placed for treatment of deep-seated tumors Tetany requires paralytics for treatment of deep-seated tumors Cardiac asynchrony requires cardiac synchronization for treatment of deep-seated tumors Difficulty overcoming impedance of epithelial tissues Limited by tumor size Potentially contra-indicated near metal implants for treatment of deep-seated tumors
IRE	Electric field threshold: >1000 V/cm Pulse duration: 50–100μs Pulse polarity: unipolar/ monophasic Pulse delivery rate: ~1 Hz or ECG synced	At least 2 monopolar probes placed parallel to each other Single needle-dual electrode Neuroparalytic/muscle relaxant: required	Requires multiple probes to be precisely placed for treatment of deep-seated tumors Tetany requires paralytics for treatment of deep-seated tumors Cardiac asynchrony requires cardiac synchronization for treatment of deep-seated tumors Difficulty overcoming impedance of epithelial tissues Limited by tumor size Contra-indicated near metal implants
H-FIRE	Electric field threshold: • Ablation: >1000 V/cm • BBBD: 113.5 V/cm Pulse width: 1–10μs Pulse polarity: bipolar/biphasic Burst delivery rate: ~1 Hz	At least 2 monopolar probes placed parallel to each other Single needle-dual electrode Single needle and surface electrode Neuroparalytic/muscle relaxant: clinicians' discretion	Requires multiple probes to be precisely placed for treatment of deep-seated tumors Limited by tumor size Contra-indicated near metal implants

[a]Miklavcic et al. (2005)
[b]Miklavcic et al. (2014)

posed by epithelial layers, thereby increasing treatment precision and minimizing the risk of skip lesions (Arena et al. 2011a). Additionally, the use of charge-balanced bipolar pulses minimizes nerve and muscle stimulation, thereby negating the need for paralytics and cardiac synchronization required during IRE delivery (Mercadal et al. 2017; Arena et al. 2011a, b).

Currently, an IRE platform is commercially available as the NanoKnife (Fig. 1b; AngioDynamics. Latham, NY, USA). The device is composed of a high-voltage

pulse generator with capabilities of pulsing across up to 6 electrode probes (not simultaneously) and can be used with a cardiac synchronization device. The generator delivers high voltage, pulsed direct current (DC) monophasic waveforms between the tips of two monopolar probes (Fig. 1c), or between the poles of a single insertion bipolar probe. Depending on the size of the lesion, insertion of multiple probes (>2) may be required to achieve complete ablation of the target tissue. IRE pulse delivery is synchronized with the patient's ECG, specifically to the absolute refractory period of the cardiac cycle, so that each pulse delivery occurs 50 ms after each R wave, to reduce the risk of inducing ventricular arrhythmias observed in earlier studies involving IRE (Thomson et al. 2011; Deodhar et al. 2011). For H-FIRE delivery, the authors use a generator commercially available through VoltMed, LLC (INSPIRE; Blacksburg, VA, USA), though many iterations of biphasic pulse generators have been proposed (Rebersek and Miklavcic 2011; Redondo et al. 2019; Elgenedy et al. 2017). Since the risk of tetany and cardiac arrhythmia induction may be reduced with H-FIRE compared to traditional IRE, cardiac synchronization is not required though remains a capability of commercial biphasic pulse generators.

In clinical settings, IRE and H-FIRE may be delivered through electrodes inserted percutaneously, endoscopically, trans-rectally, or directly into target tissues following exposure through an open surgical approach (Fig. 1d). Electrode placement is often performed under ultrasound, CT, or more recently, MRI guidance to ensure accurate placement (Collettini et al. 2019). The pulsing protocol (i.e., the number of pulses, energized time per pulse, and the locally applied electric field) dictates the electroporation effects incurred (Bhonsle et al. 2016; Pucihar et al. 2011), with reversible and irreversible electroporation treatment regimens having been described (Fig. 1d). Additionally, zones of tissue ablation can be visualized by posttreatment imaging using magnetic resonance imaging (MRI), computed tomography (CT), or ultrasonography. Due to the inherent nonthermal nature of IRE, tumor antigens and tissue components released from dying cells remain in their native form and are therefore capable of inducing a unique and robust systemic immune response. This hypothesis has been supported by evidence of DAMP signaling detected in rodent and canine models following IRE for treatment of various tumors (Ringel-Scaia et al. 2019; Brock et al. 2019).

Development of novel equipment and delivery techniques to improve treatment feasibility, efficacy, and safety have been evolving in parallel with the use of IRE for an increasing number of clinical indications. IRE delivery to cutaneous tumors historically involved the use of plate electrodes placed on either side of the tumor. Subsequent development of clinically relevant single-needle electrodes, including those with customized features such as blunted tips for use in the brain, has minimized invasiveness and improved feasibility of IRE delivery, such that these electrodes have become a standard part of the equipment used during treatment (Neal et al. 2010a). An endoscopic needle-electrode has been more recently evaluated in the porcine pancreas and determined to be feasible and effective when utilized in an endoscopic ultrasound-guided procedure. Although additional studies evaluating the safety and efficacy of this procedure are warranted, it would make endoscopic

treatment of pancreatic cancer under real-time monitoring possible and negate the need for more invasive surgical procedures. A newer technique using two spoon-shaped parallel plate electrodes (paddles) in lieu of IRE needles successfully ablated porcine pancreatic tissue when the paddles were placed around the target tissue. This technique was capable of creating a homogenous electrical field without the need for needle insertion, reducing the risk of pancreatic fistula, which has been reported in up to 18% of human patients secondary to needle tracks (Rombouts et al. 2017).

2 Treatment Planning

Treatment outcome with IRE therapies is directly influenced by exposure of target tissue to threshold electric fields. The applied electric field distribution (EFD) can be fine-tuned by altering either the PEF amplitude (500–3000 V) or the electrode configuration in which the PEFs are administered. Electrode positioning and number of electrodes, as well as length of active tip exposure, affect the EFD and therefore the ablation zone and overall treatment outcome (Wendler et al. 2016). Furthermore, though not directly affecting the EFD, parameters such as number of pulses, energized time per pulse, and pulse delivery rate can be tuned to increase the tissue's exposure to these therapeutic electric fields. An increased exposure to high electric fields is linked to a decrease in the IRE electric field threshold (Latouche et al. 2017; Siddiqui et al. 2016), therefore larger volumes of IRE can be produced. Other factors affecting treatment outcome, not under the control of the operator, include the cell type, morphology, age, and size (Gehl and Mir 1999; Miller et al. 2005). In addition, the distribution of tissue impedance can promote distortions in the applied electric fields and therefore affect ablation outcomes (Edd and Davalos 2007). Thus, pre-treatment planning using numerical methods can be used to predict the EFD throughout the target lesion prior to IRE delivery, and greatly enhance the efficacy and precision of IRE tissue ablation (Kos et al. 2015; Zupanic et al. 2012).

The EFD during electroporation can be estimated by solving a modified Laplace equation:

$$\nabla \cdot (\sigma \nabla \varphi) = 0.$$

Here, σ is the tissue electrical conductivity and φ is the electric potential. During electroporation, creation of electrically conducting defects on the cell membrane alter the bulk tissue conductivity. The change in conductivity caused by electroporation is therefore proportional to the applied PEF amplitude, which follows a sigmoidal behavior. This relationship has been characterized in skeletal muscle (Corovic et al. 2012), liver (Miklavcic et al. 2000; Zhao et al. 2018a; Bhonsle et al. 2018; Ivorra et al. 2009), prostate (Neal et al. 2014; Campelo et al. 2017), pancreas (O'Brien et al. 2019; Beitel-White et al. 2018), brain (Lorenzo et al. 2019; Garcia et al. 2010), kidney tissue (Neal et al. 2012), and other tissues (Ivorra et al. 2009; Cindric et al. 2018). Incorporation of this sigmoid–conductivity relationship captures electric field redistribution effects due to electroporation, thus informing an

accurate numerical model. Thereafter, Joule heating effects from PEF treatment are captured using a modified Pennes Bioheat transfer equation:

$$\nabla(k\nabla T) - \omega_b C_b \rho_b (T - T_a) + q''' + \frac{\sigma \cdot |E|^2 \cdot p}{\tau} = \rho C_p \frac{\partial T}{\partial t}.$$

Here, k is the thermal conductivity, ω_b is the blood perfusion rate, C_b is the blood-specific heat capacity, ρ_b is the density of blood, T_a is the arterial blood temperature, q''' is the metabolic heat generation, ρ is the density of the tissue, and C_p is the specific heat capacity of the tissue. Joule heating, resistive heating incurred from high-voltage pulsing, is dependent on the EFD as well as the on-time per pulse, p, and the pulsing period τ. Altogether, an approximation for the EFD with Joule heating effects can be accomplished using numerical methods, for example, using a finite element package like COMSOL Multiphysics (COMSOL Inc., Stockholm, Sweden). This platform can be used to develop IRE treatment plans to ensure the treatment protocol will not yield any adverse thermal effects (Edd and Davalos 2007). It should be noted, this methodology does not account for microscopic heterogeneities found in biological tissue. Tumor calcifications, tumor necrosis, large vasculature, and other critical structures embedded within the target tissue must be incorporated into the model to account for potential field distortions (Golberg et al. 2015; Ben-David et al. 2013). Lastly, once the EFD is approximated, the anticipated IRE ablation regions are determined as discrete electric field thresholds within the EFD. These thresholds can be approximated a priori using in vitro cell suspensions (Vizintin et al. 2020; Pavlin et al. 2005), in vitro tumor constructs (Dettin et al. 2019; Ivey et al. 2019; Arena et al. 2012), or determined using in vivo and ex vivo results (Corovic et al. 2012; Neal et al. 2015; Miklavcic et al. 2004). Following pulse delivery, increased cell membrane permeabilization equivalently results in increased bulk tissue conductivity; as the difference in conductivity is detectable using electrical impedance spectroscopy (EIS) methods, this change in conductivity has been the target for real-time peri-operative monitoring of treatment progression. Proposed methods for monitoring impedance changes include: (1) electrical impedance tomography, which utilizes an array of electrodes placed in/around the target tissue to reconstruct an impedance map following pulse delivery (Davalos et al. 2004); (2) electrical impedance spectroscopy to measure bulk impedance changes (Bonakdar et al. 2015; Ivorra et al. 2009); (3) using the absolute change in tissue resistance to indicate treatment cessation (Dunki-Jacobs et al. 2014); and (4) approximating the electric field distribution during pulse delivery using magnetic resonance electrical impedance tomography (MREIT) (Kranjc et al. 2017); and (5) more recently, the use of rapid EIS for continually measuring changes in tissue impedance to monitor an ablation endpoint and delineate change due to thermal and electroporation effects (Lorenzo et al. 2020). IRE-mediated cell membrane disruption results in shunting of the applied electric current throughout the target lesion, therefore successful IRE ablation will decrease tissue impedance as a result of an impaired membrane (Zhao et al. 2018b).

Altogether, the electric field distribution and the temperature distribution for a representative monopolar electrode configuration and single-insertion bipolar configuration is seen in Fig. 2 as performed in COMSOL Multiphysics v5.5. This numerical simulation was solved using electrical conductivity values of human pancreatic cancer tissue (Beitel-White et al. 2018), IRE threshold (500 V/cm) for pancreatic ductal adenocarcinoma (Arena et al. 2012) and thermal properties of healthy pancreatic tissue (O'Brien et al. 2019). The monopolar configuration was simulated as 1.5 cm spacing and 1.5 cm electrode exposure with pulsing parameters of 100 IRE pulses, applied voltage of 2500 V, 70 μs energized-time per pulse, delivered at 1 pulse per second (Fig. 2a). The bipolar configuration was simulated as 0.8 cm spacing and 0.7 cm electrode exposure, with pulsing parameters similar to the monopolar-electrode model (Fig. 2b). In this numerical model, the IRE ablation far exceeds the volume of tissue exposed to >50 °C. This numerical simulation serves to show how the electrode configuration can be modified to ablate large volumes of tissue, with minimal heating, to treat desired patient-specific tumor geometries.

Patient-specific IRE/H-FIRE treatment planning requires cross-sectional imaging of the target tissue acquired via computed tomography (CT) or magnetic resonance imaging (MRI) to generate a three-dimensional (3D) model of the target lesion (i.e., tumor) (Zupanic et al. 2012). The 3D model is then used to estimate the electric field distribution and generate a patient-specific treatment plan. Although numerical modeling computations can be completed manually, it is time consuming, so commercially available treatment planning software interfaces are often used to facilitate this process. The NanoKnife System incorporates its own touch screen software interface for basic treatment planning (not including patient imaging), procedure set-up, and real-time visualization of changes in voltage and electric current during treatment delivery. ApiVizTEP is a downloadable software application capable of generating rough estimates of the electric field distribution in real time. Web-based treatment planning software using algorithms for tissue segmentation and 3D modeling is also available that generates a downloadable treatment plan for the user (Pavliha et al. 2013). Recently, an online platform was developed to further streamline treatment planning for use with IRE treatments (Perera-Bel et al. 2020). Treatment plans provide users with information regarding probe location and spacing, electrode exposure, and delivered voltage required to achieve optimal tumor ablation while sparing adjacent normal tissue (Byron et al. 2019).

3 Limitations of IRE and H-FIRE

One of the clinical limitations of IRE is the high level of technical skill required for accurate electrode placement. Additionally, electrode positioning must be maintained during pulse delivery to ensure precise and complete treatment (Linecker et al. 2016). Risks associated with treatment are location-dependent and include hemorrhage, acute fulminant necrosis of the target tissue/organ, infection, muscle excitation, and cardiac arrhythmias. Compared to other surgical techniques,

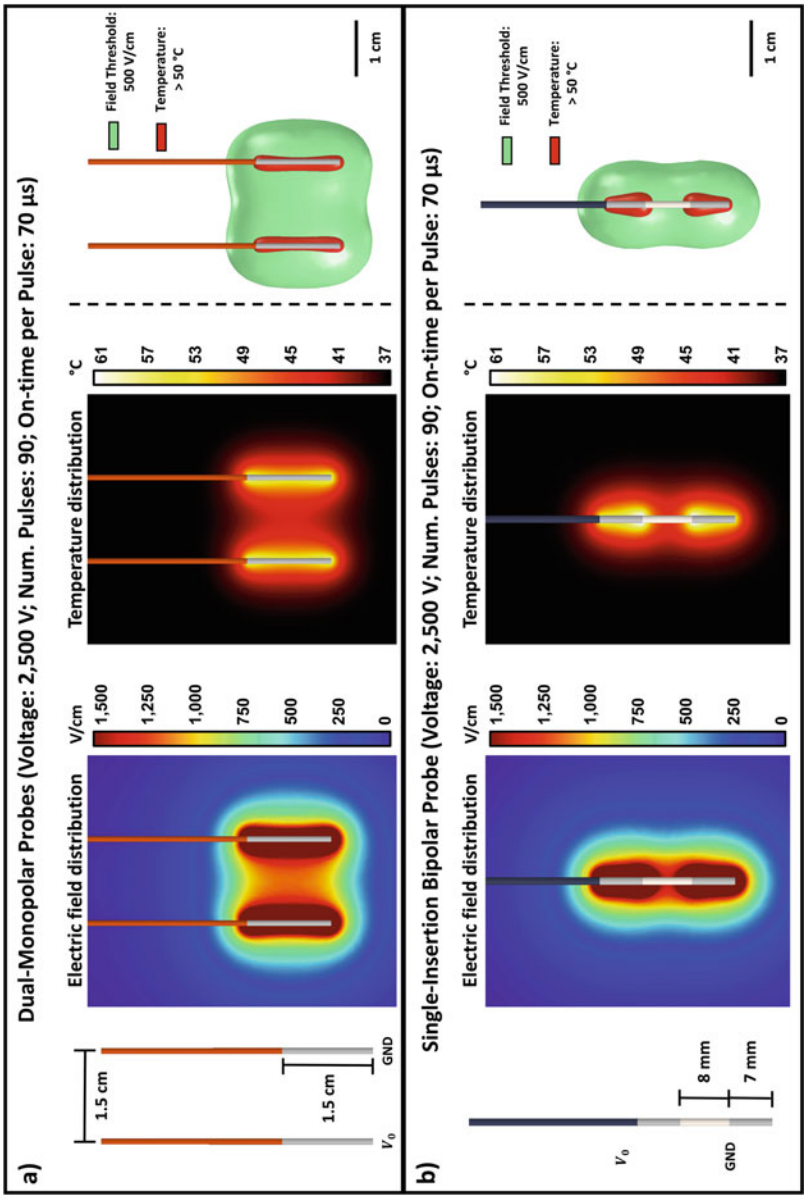

Fig. 2 Electric field and temperature distributions in monopolar and bipolar probe electrode configurations. The electric field distribution between (**a**) two monopolar electrodes and (**b**) a single-insertion bipolar probe is highest at the electrode tips and dissipates with increased distance. The temperature increase

complications are drastically lowered due to the nonthermal nature of the ablation modality with preservation of nerve function and major vasculature (Onik and Rubinsky 2010). However, the serious potential for muscle excitation and cardiac asynchrony necessitates the need for paralytics and cardiac synchronization during IRE delivery and restricts treatment eligibility to patients without underlying heart disease. In the absence of adequate neuromuscular blockade, muscle contractions associated with IRE delivery may displace implanted electrodes, thereby increasing the risk of delivering unintended electric fields to tissues and collateral damage to adjacent critical structures. These have potential for deleterious consequences, such as inadvertent damage to surrounding normal tissues (Kingham et al. 2012; Thomson et al. 2011). Furthermore, cardiac synchrony is required to avoid arrythmias. Lastly, the presence of metal, such as a stent or implant, within the ablation zone results in higher temperatures around the electrodes due to changes in electric field distribution, and is therefore contraindicated at this time (Scheffer et al. 2016).

In order to overcome some of these limitations, high-frequency irreversible electroporation (H-FIRE) was developed. H-FIRE uses ultrashort (<10 μs) bipolar PEFs that minimize nerve and muscle stimulation (Table 1). This negates the need for paralytics and cardiac synchronization, and shortens the duration of anesthetic events required for treatment procedures (Arena et al. 2011a; Ball et al. 2010). Development of a dual electrode-single needle probe compatible with currently available generators for H-FIRE delivery helped mitigate some of the technical challenges associated with multiple electrode insertions required by traditional IRE (O'Brien et al. 2019). Despite improvements in feasibility, efficacy in treating very large tumors remains limited, and research is ongoing to determine a size threshold for effective treatment.

4 Clinical Applications of IRE and H-FIRE in Companion Animals with Naturally Occurring Cancers

Veterinary patients with a variety of spontaneous cancers have served as large animal models for investigation into the feasibility and safety of IRE and H-FIRE for tumor ablation. In aggregate, these studies have indicated that IRE and H-FIRE are viable options for treatment of tumors in veterinary patients with superficial tumors (Neal et al. 2010b; Byron et al. 2019), primary liver tumors (Partridge et al. 2020), prostate cancer (Neal et al. 2014; Onik et al. 2007), and brain tumors (Garcia et al. 2010, 2012; Latouche et al. 2018; Rossmeisl et al. 2015), although clinical

Fig. 2 (continued) (resistive heating) is proportional to the applied field and is also highest near the electrode surface. At an IRE threshold of 500 V/cm, the ablation volume far exceeds a volume of tissue encompassing 50 °C. The configuration and pulsing parameters are tunable to maximize tumor cell death while sparing healthy tissue and critical structures

evidence supporting the efficacy of IRE and H-FIRE in veterinary oncology is currently limited. However, what has been demonstrated to date has been promising, and several clinical trials are ongoing. Porcine and rodent models have also been used to evaluate these technologies for treatment of pancreatic cancer (Clark 2017; Fritz et al. 2015; Charpentier et al. 2010) and mammary cancer (Ringel-Scaia et al. 2019), respectively (Table 2). Collectively, these studies support the use of IRE and H-FIRE for safe treatment of tumors located near critical structures, and particularly those that are not amenable to surgery or have failed conventional therapies.

4.1 Superficial Soft Tissue Tumors

Soft tissue sarcomas are a group of tumors arising from mesenchymal tissue that share many biological and clinical characteristics. These tumors are relatively common among veterinary patients but rarely encountered in human medicine, however, their behavior is similar across species. Important prognostic factors include tumor location, histologic subtype, tumor grade, and size (Pasquali et al. 2018). In general, these tumors tend to be very locally aggressive, forming finger-like projections, called tendrils that infiltrate surrounding tissue. The metastatic potential of these tumors greatly depends on tumor grade, with grade 1 and 2 (low-grade) tumors metastasizing in less than 15% of cases, and grade 3 (high-grade) tumors metastasizing in up to 50% of cases. Regardless of grade, most patients succumb to complications from local disease if the tumor cannot be adequately controlled via some combination of complete surgical removal and radiation therapy. Unfortunately, these tumors often form in locations not amendable to wide surgical excision, such as on the distal extremity, or in close proximity to vital structures, making wide surgical excision difficult with a high risk of morbidity and/or mortality. Thus, a nonthermal ablation method, like IRE, provides an attractive treatment option for these tumors given its ability to precisely ablate tumor tissue while sparing adjacent critical structures (Vailas et al. 2019). Current evidence supporting its application for treatment of soft tissue sarcomas in both veterinary and human patients is limited to a few case reports, making it difficult to draw significant conclusions about safety and efficacy of IRE for this purpose (Qin et al. 2017; Neal et al. 2010b; Usman et al. 2012).

IRE was successful at alleviating clinical signs associated with histiocytic sarcoma, a round cell tumor with behavior that resembles that of sarcomas, located within the left coxofemoral region in a canine patient (Neal et al. 2010b). The primary tumor was intimately associated with the sciatic nerve and femoral artery, resulting in compartment syndrome of the left thigh. Due to severe osteoarthritis, aggressive surgery involving hemipelvectomy and limb amputation was contraindicated. In this case, CT imaging was used to generate a geometric model of the target region, and a numerical model was used to determine predicted ablation zones, which were used to develop a treatment plan and pulsing protocol. IRE electrodes were placed under CT guidance, and all neurophysiologic and vascular function remained intact following treatment. Presenting clinical signs of sciatic

Table 2 Clinical applications of irreversible electroporation (IRE and H-FIRE) in veterinary patients and animal models

Application	Treatment plan	Histologic features	Adverse events	Histologic subtypes	Animal models
Superficial Soft Tissue Tumors *IRE and H-FIRE	CT-guided; percutaneous; 2-5-2 waveform in 100μs bursts; 1500–3100 V	Preservation of neurovascular structures	Depigmentation (melanoma); no clinically significant adverse effects	Histiocytic sarcoma, cutaneous tumors, melanoma	Canine[a], equine
Liver Cancer *IRE and H-FIRE	US-guided; percutaneous 1–360 pulses; 20–100μs duration; 360–3000 V/cm 2-5-2 waveform; single bipolar probe	Vasculitis; endothelial necrosis; preservation of bile ducts/vessels; well-defined ablation zones with T-cell infiltration; chronic fibrosis within ablation zone	Elevations in ALT, ALP, AST, and GGT; no clinically significant adverse effects	Normal liver, hepatocellular carcinoma	Canine, porcine, murine (rat), caprine, rabbit
Brain Cancer *IRE and H-FIRE	CT- and MR-guided; stereotactic electrode placement; intracranial via craniectomy 0–2000 V; various waveforms	Well-defined ablation zone characterized by malacia and hemorrhage; vascular preservation; microglial activation; transient BBB disruption	Coagulative necrosis and brain herniation at 2000 V/cm; seizures; peri-operative GI upset; aspiration pneumonia; hemorrhage	Normal brain, glioblastoma, meningioma	Murine, canine
Pancreatic Cancer *IRE and H-FIRE	US-guided; percutaneous; endoscopic; 100μs bursts (1/s); 80–200 s total duration; <3000 V; various waveforms; single-needle delivery	Well-defined ablation zone—interstitial hemorrhage, necrosis and edema; vascular and duct preservation; chronic—glandular atrophy and fibrosis	Elevations in ALT, amylase, and lipase; transient hypoglycemia	Normal pancreas, adenocarcinoma	Porcine

Prostate Cancer *IRE	Percutaneous or transrectal under US guidance; high-voltage steep-pulse therapy device—70 pulses of 2250 V	Distinct, well-defined lesion—complete necrosis; preservation of adjacent critical structures; resolution by 2 weeks	Muscle contraction above 1500 V	Normal prostate	Canine
Mammary Cancer *IRE and H-FIRE	200 bursts (1/s); 100μs duration 2-5-2 waveform	Well-defined ablation zone—necrosis and apoptosis; preservation of critical structures; chronic fibrosis; systemic antitumor response	Transient changes in skin color; pectoralis muscle injury	Orthotopic models (4T1), carcinoma	Porcine, rabbit, murine

[a]Single case report (Neal et al. 2010b)

Fig. 3 Regression of equine oral squamous cell carcinoma following IRE treatment. (**a**) Prior to treatment, the tumor appears as a multilobular ulcerated and necrotic lesion involving an extensive section of the buccal mucosa. There is sloughing of the necrotic ablated tumor with subsequent contraction and healing of the wound bed on days 14 (**b**), 32 (**c**), and 50 (**d**) after treatment

neuropathy and pain improved within 24 h of treatment. The ability to predict electric field distribution produced by IRE pulses through numerical modeling prior to treatment enables treatment planning for precise ablation of large, bulky tumors while sparing adjacent healthy tissue. Thus, additional research into safety and efficacy for treatment of non-resectable soft tissue tumors is warranted.

IRE and H-FIRE have been used to safely and effectively treat infiltrative superficial tumors in awake, standing horses (Byron et al. 2019). *Cutaneous tumors* are extremely common in horses, with sarcoids, squamous cell carcinoma (Fig. 3), and melanoma representing the predominant histologic subtypes. As with soft tissue sarcomas, tumors may become locally aggressive and infiltrate around critical structures, making complete surgical removal difficult (Byron et al. 2019). The current standard of care involves a combination of surgery, cryoablation, and/or intralesional chemotherapy with 5-fluoruracil or cisplatin. Despite aggressive multimodal therapy, many patients with advanced disease succumb to complications associated with their local tumor. In the aforementioned phase I clinical trial, five horses with spontaneously occurring multifocal cutaneous tumors were treated with H-FIRE every 2 weeks for 2–4 outpatient visits. H-FIRE was delivered as a 2-5-2 μs burst scheme (positive phase-, intraphase delay-, negative phase) with each burst energized for 100 μs and an applied voltage between 1500 and 3100 V. Treatment was successfully delivered to all horses on an outpatient basis, without the need for general anesthesia or neuromuscular blockade. All patients tolerated treatment well with no reported complications. A significant decrease in tumor volume was noted in all horses, and tumor ablation was confirmed on ultrasound and histologic examination. Additionally, depigmentation of skin occurred within treatment zones of melanomas, suggesting effective ablation of melanocytes. Thus, H-FIRE appears to be a clinically feasible, safe, and potentially effective outpatient treatment option for management of superficial tumors, however, multiple treatments may be necessary to adequately treat large tumors.

4.2 Liver Cancer

Primary liver tumors are the third most common cause of cancer related death in people. Surgical resection is the most effective treatment for the predominant

histologic subtype, hepatocellular carcinoma (HCC), however, this is only feasible for about 40% of patients due to the presence of advanced disease at the time of diagnosis in the majority of cases (Balogh et al. 2016). Aside from liver transplantation, effective alternative treatment options are limited, thus non-resectable tumors have historically carried a grave prognosis.

HCC is also fairly common in dogs and represents the predominant histologic subtype of primary liver tumors. Compared to HCC in people, tumors are resectable in about 60% of canine patients; however, non-resectable tumors mirror their human counterparts (Kinsey et al. 2015; Liptak et al. 2004). The majority of canine HCCs arise from a single liver lobe (massive form), however, large tumors arising from the right side of the liver and/or those in close proximity to the hilus can rarely be removed completely without compromising vital structures. Thus, limited alternative treatment options exist for these patients despite the absence of disseminated disease. Canine HCC has served as a model for investigation into novel therapies, such as IRE, specifically H-FIRE, for treatment of non-resectable liver tumors. Given the potential for IRE to induce a unique, yet robust, antitumor immune response, the liver became of particular interest because of its immunologically rich but tolerogenic environment (Robinson et al. 2016).

Percutaneous irreversible electroporation (IRE) has been evaluated in people bearing primary and secondary liver tumors and appears to be well tolerated (Scheffer et al. 2014b; Narayanan 2015). IRE has been successfully used to ablate tumors intimately associated with the biliary tract without damaging bile ducts (Silk et al. 2014). This makes it an attractive treatment option for centrally located liver tumors, which typically lie next to major bile ducts. Likewise, safety of IRE for treatment of tumors near or encasing major vessels has been demonstrated (Narayanan et al. 2014). Adverse effects reported in the literature include liver abscess formation (4–5%), hemorrhage (typically self-limiting), subcapsular hematoma formation, kidney failure, pneumothorax, mild pleural effusion, hepatic arteriovenous shunt formation (3.5%), partial portal vein thrombosis, atrial fibrillation, and transient neurologic signs affecting the right thoracic limb (2.3%) (Kalra et al. 2019; Mafeld et al. 2019; Dollinger et al. 2015; Bhutiani et al. 2016). Significant, yet transient, elevations in alanine transaminase (ALT) and aspartate transaminase (AST) have been reported 1–2 days following treatment, returning to baseline within approximately 2 weeks. Similarly, significant elevations in total and direct bilirubin levels have been detected 8–10 days following treatment, returning to baseline within 2 weeks (Alnaggar et al. 2018).

Based on completed studies, treatment efficacy and clinical outcome are dependent on completeness of tumor ablation, tumor recurrence, local recurrence-free survival (LRFS), and progression-free survival (Tameez Ud Din et al. 2019). Complete ablation rates vary by study, but are generally higher in medium-sized tumors (66%) compared to large tumors (25%) (Kalra et al. 2019; Zeng et al. 2017). Local recurrence has been observed in 21% of patients at 3 months and 31–34% of patients at 6 months and beyond (Niessen et al. 2017; Fruhling et al. 2017; Saini et al. 2018). The overall median survival time of patients experiencing local recurrence is 26.3 months. Based on currently available data, 87–97% of patients remain disease

free at 3 months, 78–94% remain disease free at 6 months, and 59–75% of patients remain disease free at 12 months following treatment. LRFS improved significantly for tumors measuring less than 3 cm as 100% of patients were free of disease at 3 and 6 months, and 98% of patients free of disease at 12 months (Cannon et al. 2013; Niessen et al. 2016). The median overall progression-free survival following IRE alone is 7–9 months, longer for smaller tumors (Kalra et al. 2019; Sutter et al. 2017). The reported median survival time following IRE is approximately 26.8 months for primary liver tumors and 19.9 months for secondary liver tumors, with overweight patients and those with tumors >3 cm or >3 lesions having a worse prognosis (Saini et al. 2018). Tumors larger than 5 cm often fail to respond favorably to IRE (Thomson et al. 2011). Thus, the utility of IRE may involve treating smaller (<3 cm), residual lesions within the liver following resection of the primary tumor. Additionally, IRE has been successful at down-staging patients after initial surgery to facilitate the second portion of a two-staged hepatectomy (Langan et al. 2017).

Preliminary studies evaluating the effects of IRE on liver tissue were performed using various animal models, including pigs, rats, goats, and rabbits. All animals in all studies survived the immediate treatment and posttreatment period (Vogel et al. 2019). Applied pulse parameters varied from 1 to 360 pulses of 20–100 μs duration delivered at 360–3000 V/cm. Similar to people, acute transient increases in ALT and AST were observed starting as early as 1 h after treatment and resolving within 2 weeks after treatment (Charpentier et al. 2011; Au et al. 2011). IRE produced well-demarcated ablation zones of variable diameter as early as 90 min after treatment (Appelbaum et al. 2012, 2014; Ben-David et al. 2012). Ablation zone size appears to be significantly associated with electrode size, inter-electrode distance, and electric field strength (Miklavcic et al. 2000). Vasculitis and endothelial necrosis with preservation of nearby bile ducts and vessels were observed in gross and histologic liver samples following treatment, which is consistent with IRE-induced changes described in other organs (Liu et al. 2012; Schmidt et al. 2012). Progression of histologic events resembles that observed in other organs, with necrosis, hemorrhage, vascular congestion, and mononuclear inflammation predominating over the first 24–48 h after treatment, which resolve by two weeks post-treatment and become completely replaced by fibrous scar tissue (Guo et al. 2011; Lee et al. 2012).

High-frequency irreversible electroporation (H-FIRE) has been evaluated in a porcine liver model in which it induced rapid, predictable ablations without the need for intraoperative paralytics or cardiac synchronization. H-FIRE electrodes were inserted 1.5 cm apart with ultrasound guidance, and ablations were performed using 100, 200, or 300 bursts with a 2-5-2 μs burst scheme and an applied voltage 2250 V. Hepatic ablations were intentionally planned across, or adjacent to, critical vascular and biliary structures. Minor muscle twitching was observed but no other clinically significant adverse effects. Porcine livers were resected 6 h after treatment for histologic evaluation. Reproducible ablation volumes were observed at necropsy, with apoptosis predominating within the lesions treated with <200 pulses. Necrosis predominated in lesions treated with >200 pulses (Siddiqui et al. 2016). In all lesions, minor endothelial damage was observed, while vascular and biliary

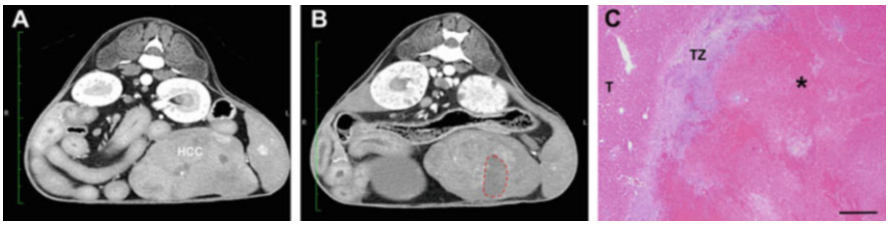

Fig. 4 H-FIRE ablation of canine hepatocellular carcinoma (HCC). Post-contrast CT scans of the HCC prior to (**a**) and following H-FIRE treatment (**b**), with a well-demarcated ablative lesion appearing as a hypoattenuating region in **b** (red dashes). Photomicrograph (**c**) illustrating the well-demarcated ablation zone (*) separated from untreated tumor (T) by a transition zone (TZ); H&E, bar = 500μm

structures remained structurally intact. Given the improved clinical feasibility of H-FIRE delivery compared to IRE it may be the preferred ablation method for various tumor types that are not amenable to surgical removal (Siddiqui et al. 2016).

The safety and feasibility of percutaneous H-FIRE were evaluated in a pilot study involving three canine HCC patients. H-FIRE was delivered through a bipolar probe that was percutaneously placed into the center of tumor under ultrasound guidance. Treatment delivery involved a 2-5-2 μs H-FIRE burst scheme, 300 bursts delivered at 1 burst per second, 100 μs energized time per burst, and an applied voltage of 2250 V. Treatment delivery was completed under general anesthesia without the use of paralytics or cardiac synchronization. No treatment-related adverse effects were observed during treatment delivery or the immediate posttreatment period. CT imaging performed 4 days post-treatment revealed a well-defined ablation zone within the tumor that corresponded with gross findings following tumor resection (Fig. 4). Histologically, H-FIRE produced a well-defined ablation/tumor interface characterized by CD3+ lymphocyte infiltration. Interestingly, infiltrating lymphocytes were negative for CD4 and CD8, and CD79a+ lymphocytes were not observed. CD3+/CD4-/CD8- lymphocytes have previously been associated with immune regulation and tolerance (Martina et al. 2015; Ford et al. 2002). Given that the liver is an immunologically rich microenvironment, these lymphocytes may serve to recognize tumor antigens released in their native form following H-FIRE-induced cell death (Partridge et al. 2020).

Overall, no clinically significant adverse effects were observed throughout the study period, supporting the safety and feasibility of H-FIRE for treatment of non-resectable liver tumors. Elevations in liver enzymes (ALT and ALP) above baseline occurred following H-FIRE delivery but resolved over time following tumor removal. Additional investigation into the efficacy of H-FIRE as a treatment for non-resectable liver tumors is currently ongoing. In general, canine HCC patients present with relatively large primary tumors unless identified incidentally while small. Given the risk of tumor rupture and subsequent life-threatening hemorrhage if left in place, a more practical approach may involve H-FIRE delivery to residual gross and/or microscopic disease following incomplete resection of bulky disease.

Investigation into the efficacy of H-FIRE for residual and/or non-resectable liver tumors is currently ongoing. Additionally, further characterization of the systemic immune response to H-FIRE delivery within the liver is warranted (Partridge et al. 2020).

4.3 Brain Cancer

Glioblastoma (GBM) is the most common and deadliest of the malignant primary brain tumors affecting humans. These tumors are incredibly aggressive and neuroinvasive, making complete surgical removal nearly impossible. Additionally, its location behind the blood–brain barrier prevents effective delivery of most therapeutics. Thus, GBM carries a grave prognosis with median survival times following a combination of aggressive surgery, radiation, and chemotherapy of only 14–16 months, and a 5-year survival rate of about 5% (Stupp et al. 2005; Tamimi and Juweid 2017). Canine and humans are the only species that commonly develop malignant gliomas, and a number of clinicopathological and genomic characteristics of these tumors are shared across species, thus dogs are an excellent large animal model for investigation into novel therapies for malignant glioma.

Glioblastomas are capable of creating a highly immunosuppressive microenvironment, allowing them to evade the immune system, further promoting tumor progression. Decreased MHC expression by tumor cells limits self-presentation of antigens, and PDL1 expression binds to PD1 on effector cells and silences immune system activation. Tumor cells also produce chemokines that recruit regulatory T-cells, tumor-associated macrophages and myeloid-derived suppressor cells, which further suppress the immune system and promote tumor growth. Lastly, resident microglial cells within the microenvironment express immunosuppressive factors, such as TGFβ and IL-10, that suppress local and systemic immune responses, ultimately disrupting systemic tumor antigen detection and immune system activation (Chen and Hambardzumyan 2018; Lim et al. 2018). IRE seems capable of transforming the immunosuppressive, tumor-promoting microenvironment associated with these tumors to an antitumor pro-inflammatory microenvironment by inducing damage-associated molecular pattern (DAMP) signaling in ablated cells. In contrast to thermal ablation methods, the nonthermal nature of IRE allows for release of tumor antigens in their native form, unaltered by heat or cold, and is, therefore, more likely to induce a robust systemic immune response. Such local and systemic immune system activation may be capable of inducing tumor cell death within distant lesions (Ringel-Scaia et al. 2019).

Following a single treatment, IRE induces a central zone of irreversible electroporation surrounded by a zone of reversible electroporation, providing an opportunity to therapeutically target the penumbra of microscopic disease, which is a major source of disease recurrence (Arena et al. 2011a). More specifically, in the needle electrode configuration, the reversible regime occurs at lower electric field thresholds and thus will always encase the IRE tissue ablation volume. This penumbra extends centimeters beyond the zone of IRE and coincides with the outer zone of

reversible electroporation, thus following a single IRE delivery, microscopic cells within this zone undergo transient membrane permeabilization, whereas cells comprising the gross tumor are ablated. Thus, this technology may be exploited further with adjuvant electrochemotherapy to target microscopic cells within the penumbra (outside the ablation zone) and potentially improve long-term outcomes. Furthermore, additional improvements in clinical outcomes may be achieved by delivering adjuvant electrochemotherapy to microscopic tumor cells residing within adjacent grossly normal brain tissue following tumor resection. Lastly, this technology could be used to intentionally and reversibly disrupt the blood–brain barrier to deliver therapeutic agents that would otherwise be impermeant to the CNS (Sharabi et al. 2020). As the thresholds for BBB permeabilization have been shown to be significantly lower than that of irreversible electroporation, the opportunity to disrupt the BBB while fine-tuning the desired extent of tissue ablation is feasible with IRE and H-FIRE therapies. In addition, a delineation between reversible electroporation and BBB disruption has been demonstrated in vitro, thereby presenting the opportunity for BBB disruption at very low electric fields with minimal to no reversible electroporation effects (Sharabi et al. 2019).

To date, research investigating IRE and H-FIRE for treatment of brain tumors has been limited to rodent and canine models as further characterization of its local and systemic effects is required prior to translating it for treatment of primary brain tumors in people (Garcia et al. 2012). The safety and feasibility of intracranial IRE were first evaluated in five normal research bred dogs (Ellis et al. 2011). IRE was delivered to the cerebrum at various pulse parameters followed by intra-operative ultrasound and postoperative MRI to visualize the ablation zones and treatment associated blood–brain barrier disruption (BBBD; Fig. 5a). In order to study the upper safety limit of the procedure, one dog received a higher total voltage, and subsequently experienced coagulative necrosis of all tissues within the treatment field and clinical signs of brain herniation within 14 h of treatment. This dog was humanely euthanized, but no other dogs experienced significant deterioration in neurologic function from baseline or seizure activity. All dogs were humanely euthanized 3 days after treatment to evaluate IRE-induced histologic changes. Gross pathologic findings included a well-demarcated region of malacia and intraparenchymal hemorrhage, which corresponded to changes present on posttreatment MRI. Histologically, a sharp demarcation between the ablation zone and transition zone, the submillimeter region located between the ablation zone and normal brain, was evident, with preservation of major blood vessels located within the ablation zone itself (Rossmeisl et al. 2015). Additionally, parenchymal vacuolization and astrogliosis was noted following delivery of higher voltage. The DAMP protein, high mobility group box 1 (HMGB1) was detectable in all dogs with increased amounts present within the IRE lesion itself compared to the adjacent transition zone, increasing directly with electric field strength (Fig. 5b). Immunohistochemistry with IBA-1 for resident microglia revealed an increase in microglial size within the zone of transition compared to normal brain, which has previously been associated with microglial activation. Evidence of a cell-mediated immune response was limited as minimal T-cell infiltration occurred within the transition zone, but this

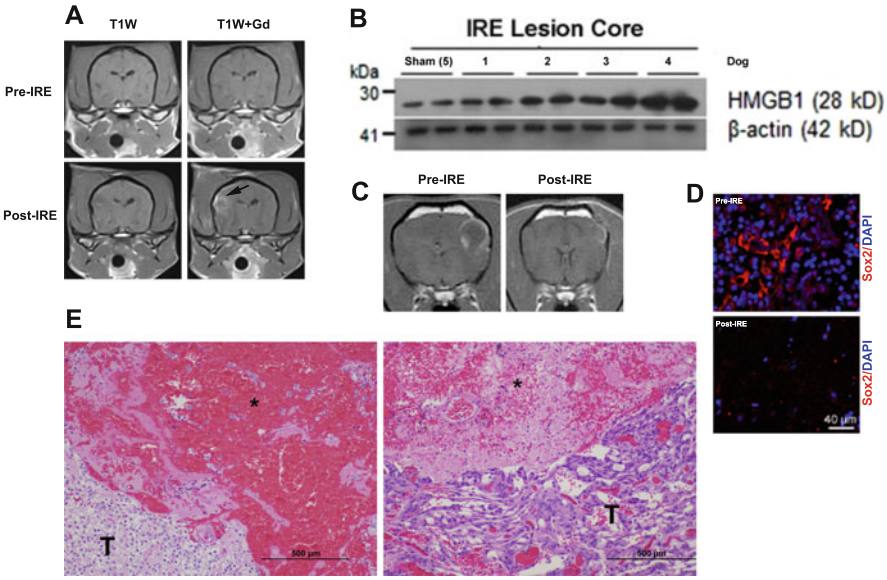

Fig. 5 Effects of IRE and H-FIRE treatments in the canine brain. (**a**) IRE treatment of normal brain results in blood–brain barrier disruption as indicated by the presence of contrast-enhancement of the brain parenchyma (arrow) in the treated region on MRI. (**b**) Western blot demonstrating increased expression of the DAMP protein, high mobility group box 1 (HMGB1), in the brains of all dogs treated with IRE compared to sham operated control. (**c**) MRI demonstrating ring-enhancing astrocytoma in the brain (left) with complete response after IRE treatment, as evidenced by complete disappearance of the tumor (right). (**d**) Pretreatment biopsy (top) of a canine glioblastoma revealing SOX2 positive glioma stem-like cells (GSC); following IRE treatment (bottom) the GSC are ablated. (**e**) IRE (left; GBM) and H-FIRE (right; meningioma) produce ablations that are sharply demarcated from untreated tumor (T); H&E, bar = 500µm

is likely due to the temporal confines of the study preventing detection of a robust cell-mediated immune response (unpublished data). Results of this study suggest that when used at appropriate pulse parameters, IRE is a safe and feasible ablation method for use within the brain and capable of inducing DAMP signaling.

A subsequent clinical trial was completed to evaluate the safety and feasibility of IRE for the treatment of canine intracranial gliomas (Rossmeisl et al. 2015). Seven client-owned dogs with spontaneous gliomas were treated with IRE delivered under CT-guidance. A posttreatment CT was performed immediately after treatment to visualize tumor ablation. Significant adverse events occurred in two dogs, one of which had aspiration pneumonia that was unlikely directly related to IRE and more likely related to the craniectomy, as it is a known risk of this procedure. The remaining dog received an unexpectedly high dose of energy due to pulse delivery to the ventricular system and increased conductivity of the cerebrospinal fluid compared to tumor tissue. The median duration of hospitalization was 4 days, and Karnofsky Performance Scores, which assesses functional impairment, improved in all dogs that survived to discharge by two weeks following treatment. Likewise,

improvement in seizure control was noted in five dogs. Based on RANO criteria, 80% of dogs with a quantifiable target lesion responded to IRE treatment, defined as stable disease (1), partial response (2), and complete remission (1, Fig. 5c) (Garcia et al. 2017). The overall median survival time of these patients was 119 days with two patients completing the 12-month follow-up. Histologic evaluation of the treated lesion from the dog that unexpectedly died of aspiration pneumonia revealed a sharp delineation between ablated tumor and surrounding brain (Fig. 5e) with a visible transition zone between the lesion and normal brain characterized by vacuolated neuropil and perivascular inflammatory cuffing. Additionally, immunofluorescent staining with the neural stem cell marker, SOX2, revealed selective ablation of glioma stem-like cells following IRE treatment compared to pre-treatment biopsy samples, suggesting that IRE may be capable of eliminating glioma-like stem cells which are often implicated in treatment failure and subsequent tumor recurrence (Fig. 5d). These findings provide evidence that the treatment plan designed to ablate the entire tumor was effective at treating the tumor without causing significant collateral brain damage. Given the results of this study, IRE seems to be a safe and feasibly treatment option for canine gliomas.

We have shifted our research focus toward H-FIRE technology since its development. H-FIRE was able to successfully ablate brain tissue and transiently disrupt the blood–brain barrier within the penumbra of tissue surrounding the ablation zone in rodent models without causing muscular contractions (Arena et al. 2011a, b). This novel technique was introduced as a potential treatment for spontaneous brain tumors in a feasibility study evaluating H-FIRE in dogs with intracranial meningioma (Latouche et al. 2018). Three dogs with intracranial meningioma were treated using patient-specific treatment plans generated based on MRI imaging. H-FIRE was stereotactically delivered to all patients followed by a posttreatment MRI and tumor resection to characterize histologic changes. H-FIRE delivery was successful in all patients without any adverse events directly related to H-FIRE treatment. One dog experienced intraoperative hemorrhage and subsequent hypotension during tumor resection and developed worsening of neurologic signs postoperatively, but recovered and was discharged with improvement in neurologic signs by 2 weeks posttreatment. No intra- or postoperative adverse effects were observed in either of the remaining dogs. Posttreatment MRI revealed a well-demarcated homogenous region of ablation characterized by complete disruption of tumor architecture with tumor necrosis volumes measuring 0.25–1.29 cm^3. In one dog, posttreatment histopathology revealed nonuniform ablations with viable tumor cells persisting around foci of intra-tumoral mineralization. This suggests that intra-tumoral mineralization may limit the ability of H-FIRE to produce complete, homogenous tumor ablation. Results of this study support the use of H-FIRE for the treatment of brain tumors based on its ability to safely produce clinically relevant volumes of tumor ablation without muscular contraction or cardiac arrhythmias.

Current research into the mechanism of H-FIRE mediated blood–brain barrier disruption (BBBD) as well as the local and systemic immune response to H-FIRE in normal brain and those affected by glioma are ongoing. A study evaluating H-FIRE in normal rat brains provided evidence of H-FIRE induced transient blood–brain

barrier disruption at electrical field strengths significantly less than those required to ablate tumor tissue (Lorenzo et al. 2019). MRI performed at various time points following H-FIRE delivery revealed an increase in contrast enhancement at the site of H-FIRE delivery 1-hour post-treatment compared to the sham control, followed by a gradual decrease in contrast enhancement over time consistent with blood–brain barrier repair. This correlated with gross pathologic findings, where an increase in Evan's Blue Dye was noted within the brain parenchyma 1 hour following treatment compared to the sham control, followed by a gradual decrease over time. Histologically, H-FIRE lesions were limited to mechanical damage associated with the electrode insertion tract, where lesions did not differ between treatment and control groups. An influx of inflammatory cells was noted at 48 and 96 h but there was no visible damage to the surrounding brain parenchyma. In contrast, large, necrotic lesions were present within the brain parenchyma surrounding lesions created by higher, more ablative doses. Results of these preliminary studies indicate that H-FIRE transiently permeates the blood–brain barrier without disrupting adjacent normal brain tissue. A more realistic application of this technology is for the treatment of residual microscopic disease following surgical removal of gross tumor tissue. The ability of H-FIRE to induce transient BBB disruption and create a surrounding zone of reversible electroporation that coincides with the penumbra of microscopic disease may be exploited to treat residual microscopic disease and delay tumor recurrence. Additionally, H-FIRE induced BBBD could aid in the delivery of chemotherapeutics that would otherwise be excluded from the CNS by an intact BBB.

Intracranial H-FIRE has been successfully delivered under MRI guidance in canine patients with gliomas without any treatment-associated complications. An increase in gadolinium contrast enhancement following H-FIRE treatment was observed, which corresponded to the amount of BBBD in these patients. Thus, H-FIRE induced BBBD has been successfully achieved in tumor-bearing dogs, but further investigations into its safety and efficacy are ongoing. Additionally, ongoing experiments aim to better characterize the local and systemic immune responses to intracranial H-FIRE and assess its efficacy when used alone or with a molecular adjuvant as a combinatorial approach for treatment of gliomas.

5 Clinical Applications of IRE and H-FIRE in Preclinical Normal Animal Models or Experimentally Induced Tumors

5.1 Pancreatic Cancer

Pancreatic adenocarcinoma is the deadliest of cancers affecting the gastrointestinal tract with less than 5% of people surviving 5 years despite aggressive therapy (Siegel et al. 2017). Many people are asymptomatic during early stages of the disease, making early detection difficult. At the time of diagnosis, 50% of patients have metastatic disease and only 20% of patients are candidates for surgery (Callery et al. 2009). Given its location within the pancreas, locally advanced disease often

involves nearby structures, such as major vessels. Surgical resection in these cases is associated with high perioperative morbidity and mortality, while only minimally impacting survival (Kato et al. 2013; Chua and Saxena 2010). The prognosis for people with non-resectable tumors is grave, with an overall median survival time of 9–13 months despite treatment with chemotherapy and/or radiation therapy (Kane and Knox 2018).

Pancreatic carcinomas are uncommonly diagnosed in veterinary medicine, but their clinical presentation and response to treatment parallels that described in people (Priester 1974). Clinical signs are non-specific and may include some combination of lethargy, anorexia, vomiting, diarrhea, polyuria, polydipsia, and/or a palpable mid-abdominal mass. By the time veterinary patients become clinical for their disease, it is often advanced with local invasion into adjacent structures and metastasis to the regional lymph nodes, liver, intestine, and/or lungs. Surgical resection is rarely possible at the time of diagnosis due to advanced stage of disease; so many patients are humanely euthanized without further treatment. Reported survival times vary, with most patients succumbing to disease within days to months following diagnosis despite treatment with chemotherapy and/or radiation therapy (Aupperle-Lellbach et al. 2019; Pinard et al. 2020). No currently available treatments have been shown to significantly prolong survival of veterinary patients with pancreatic carcinoma, thus the need for novel treatment options is undeniable.

IRE has emerged as an attractive ablation method for treatment of non-resectable pancreatic tumors. Since IRE does not rely on heat for effective tumor ablation, adjacent critical structural components are spared and it can be used in proximity to large vessels without compromising efficacy due to the "heat sink effect" (Davalos et al. 2015). Given the proximity of the pancreas to critical vascular structures, including but not limited to arterial and venous vessels, bile and pancreatic ducts, nerves, and adjacent organs, IRE may be used to effectively ablate locally advanced tumors without the unintentional collateral damage that typically occurs during attempts at surgical resection. Unlike IRE ablations in other organs, real-time ultrasound imaging during IRE delivery to the pancreas is limited due to formation of edema, which obscures the field (Rubinsky et al. 2007). Recent development of pre-treatment planning models helps predict ablation volumes and ensures precise IRE delivery and subsequent tumor ablation (Latouche et al. 2017).

Clinical trials evaluating the use of IRE in patients with late-stage, locally advanced pancreatic adenocarcinoma have shown promising results. The reported median overall survival time is 7–23 months post-treatment with longest survival times reported in patients undergoing a combination of IRE and surgical resection (Ansari et al. 2017). These survival times surpass those reported for patients receiving traditional therapies and treatment-associated complication rates are significantly lower than those associated with other ablation methods (Scheffer et al. 2014a). IRE is not only capable of safely ablating locally invasive tumors, but appears to induce a pro-inflammatory microenvironment that promotes immune cell infiltration into the tumor, further halting tumor progression. Additionally, since IRE ablates cancer cells without heat, tumor antigens released from the

dying cells are preserved and may induce an antitumor immune response against residual and metastatic cells (Brock et al. 2019).

Veterinary patients have historically been utilized as models to investigate the feasibility and safety of IRE in pancreatic tissue. Porcine models predominate as their pancreatic anatomy and physiology parallels that of humans and small animal veterinary patients. Studies evaluating IRE in pancreatic porcine models have shown this technique to be feasible and safe (Fritz et al. 2015; Bower et al. 2011; Charpentier et al. 2010; Wimmer et al. 2013). A study evaluating the safety and ablation volume of IRE in a porcine pancreas model showed that IRE is well tolerated when performed at an optimal voltage of 3 kV. Ultrasound was utilized to guide electrodes within 1 mm of the portal vein or mesenteric artery. All animals recovered with only mild adhesions but no pancreatic necrosis, ascites, or hemorrhage, which have been reported in other studies (Bower et al. 2011; Fritz et al. 2015; Wimmer et al. 2013). Elevations in ALT levels and transient hypoglycemia were also noted in these patients immediately after treatment but resolved over 24 h. IRE resulted in a 3 cm × 2.8 cm ablation zone characterized by significant destruction of pancreatic tissue with the exception of spared, intact vasculature (Bower et al. 2011). These histologic findings parallel those described in other studies, particularly with regards to preservation of blood vessels and pancreatic ducts among hemorrhagic necrosis of the pancreatic interstitium (Charpentier et al. 2010; Fritz et al. 2015). In another study, IRE was delivered to the pancreatic tail in pigs that were terminated after 60 min, whereas it was delivered to the head of the pancreas in a separate cohort of pigs that were observed for 7 days. In this study, no cardiac abnormalities, signs of acute pancreatitis nor other clinically significant adverse effects were observed. CT performed 60 min after treatment revealed the presence of a hypodense lesion corresponding with the ablation zone (Fritz et al. 2015). Transient increases in amylase and lipase is frequently reported as a side effect of IRE treatment within the pancreas, typically peaking after 24 h and resolving within 2–3 days (Fritz et al. 2015; Bower et al. 2011; Vogel et al. 2019). Histologically, acute lesions observed within 1 hour of treatment appear sharply demarcated with interstitial edema and mild hemorrhage. Over time, inflammatory infiltrates contribute to fibrosis and glandular atrophy and signs of apoptosis and necrosis become evident. Autolytic changes become apparent approximately two weeks after treatment with progression to extensive fibrosis and acinar atrophy within the ablation zone after 1 month.

H-FIRE was evaluated for pancreatic tissue ablation using 100 μs energized bursts delivered at 1 burst/second for 80–200 bursts to successfully ablate porcine pancreatic tissue without inducing muscle tetany or cardiac arrhythmias (Clark 2017). As with IRE, treatment zones were visible on intraoperative ultrasound and posttreatment CT. Another study successfully delivered H-FIRE through a single-needle delivery approach in swine pancreas without concurrent use of intraoperative paralytics or cardiac synchronization (O'Brien et al. 2019). Three different waveforms (1-5-1, 2-5-2, and 5-5-5 μs burst schemes) were used with a total energized time of 100 μs per burst resulting in a significant increase in mean ablation area with increasing pulse width. No clinically significant adverse effects were noted and the lethal threshold for pancreatic tissue varied between voltage waveforms, but

ranged from 693 to 1114 V/cm. Immunohistochemical staining for cleaved caspase-3 was absent from the ablation zone; however, the extent of positive staining was significantly different between voltage waveforms. These findings suggest H-FIRE-induced cell death likely occurs through mechanisms other than apoptosis, which have been highlighted through various studies evaluating IRE in other organs.

Immunotherapy has shown significant promise in cancer treatment for many tumor types, but its efficacy in pancreatic cancer is limited by the presence of a highly fibrotic stroma, which creates an immunosuppressive tumor microenvironment by physically preventing cytotoxic T-cell infiltration (Thind et al. 2017). IRE appears capable of transforming this immunosuppressive tumor microenvironment to a pro-inflammatory antitumor microenvironment by inducing immunogenic cell death and dendritic cell activation (Zhao et al. 2019). When combined with anti-programmed cell death protein 1 (anti-PD1) immune checkpoint blockade, tumor infiltration by CD8+ T-cells occurs and a long-term memory immune response has been documented in a murine orthotopic pancreatic cancer model (Zhao et al. 2019). Thus, IRE may be exploited to improve response to checkpoint inhibitors and overall outcome in people with pancreatic cancer. Currently, checkpoint inhibitors are not available for use in small animal veterinary patients, but development is ongoing and response to combination therapy is expected to yield similar results.

5.2 Prostate Cancer

The incidence of *prostate cancer* in people is on the rise with more than a million new cases diagnosed each year. Men aged 65 years and older have the highest risk, thus annual screening is recommended at ages 45 years and above (Rawla 2019; Guenther et al. 2019). Currently, the available treatment options include radical prostatectomy, radiation therapy of the entire prostate, and chemotherapy. Treatment frequently results in physically and emotionally debilitating side effects, such as impotence and incontinence, with damage to the rectum and bladder also possible (Guenther et al. 2019). The survival benefit of aggressive multimodal therapy is modest compared to active surveillance alone, thus a need for effective, well-tolerated treatment options currently exists for management of this disease (Bill-Axelson et al. 2018). The incidence of prostate cancer in veterinary patients is much lower but these patients often present with advanced disease, including osteoblastic bone metastases, which are common in people. Similar challenges are faced when treating prostate cancer in veterinary patients, with most patients succumbing to local disease progression within a year despite aggressive therapy (Leroy and Northrup 2009). Noninvasive thermal ablation methods, such as radiofrequency ablation and high intensity focused ultrasound (HIFU) are increasing in popularity, but the efficacy and adverse effects are influenced by the “heat sink” effect. In contrast, the nonthermal mechanism by which IRE induces cell death allows improved treatment precision and spares adjacent critical structures. Given the prostate is closely associated with many critical structures, including the components

of the urinary tract, rectum, and neurovascular bundles, treatment precision is imperative to eliminate adverse effects.

In people, the clinical feasibility and safety of IRE for treatment of prostatic carcinoma have been established (van den Bos et al. 2016). Outcomes following treatment with IRE for prostatic carcinoma parallel those following radical prostatectomy but are associated with less urogenital dysfunction. A study evaluating transrectal IRE in 34 human patients with prostatic carcinoma reported only mild (grades 1 and 2) complications within a 6-month follow-up period. All patients remained continent and only 5% of patients experienced impotence (Valerio et al. 2014). The utility of IRE ranges from focal tumor to whole-gland ablation, and may provide a safe, alternative treatment option for large tumors that are no longer amenable to surgery and radiation therapy (Guenther et al. 2019).

IRE treatment of prostatic tissue was first evaluated in 6 normal dogs. IRE probes were placed percutaneously or transrectally under ultrasound guidance for delivery and patients were followed for up to 2 weeks. The rectum, urethra and neurovascular bundle were intentionally targeted in a single dog to assess the impact of treatment on these structures. Patients experienced variable degrees of muscle contraction, with the severity of contractions increasing with applied voltage, however, voltages less than 1.5 kV produced minimal contraction. This likely reflects the voltage that would be applied in a clinical setting, as it appears to successfully ablate prostatic tissue without adverse effects. IRE resulted in a distinct, well-demarcated lesion characterized by complete necrosis and a narrow zone of transition from the ablation zone to normal tissue. Adjacent critical structures appeared unaffected by treatment, and near resolution of the lesions occurred within two weeks. Similar histologic lesions with preservation of adjacent neurovasculature have been reported in human patients following IRE for treatment of prostatic carcinoma, thus IRE appears to be a safe and potentially effective treatment option for prostate cancer (Onik et al. 2007; van den Bos et al. 2016).

Traditionally, IRE has been delivered through the commercially available NanoKnife system. Recently, a novel high-voltage steep-pulse therapy device was developed for ablation of prostatic tissue and evaluated in normal dogs. Two electrode probes were used to deliver IRE under real-time ultrasound guidance. Seventy pulses of 2250 V were delivered to each dog with no serious complications. Treatment resulted in a sharply demarcated ablation zone with preservation of the urethra and adjacent blood vessels, consistent with previous studies (Han 2019). Research into the efficacy of IRE for treatment of canine prostatic carcinoma is currently lacking, but based on its safety and efficacy in human patients, promising results are to be expected.

5.3 Mammary Cancer

Breast cancer is the second most common cancer in women, following closely behind skin cancer. Treatment and prognosis are frequently influenced by the presence of estrogen receptor alpha (ERa), progesterone receptor (PR), and human

epidermal growth factor receptor 2 (HER2) expressions (Rakha et al. 2010). Triple-negative breast cancers (TNBCs), which fail to express ERa, PR, and HER2 have been associated with a poor prognosis due to the current lack of effective targeted therapy (Bianchini et al. 2016). Mammary carcinomas in veterinary medicine share a number of clinical, epidemiologic, and pathologic features with their human counterpart. In dogs, triple-negative mammary carcinomas predominate (76%) and the aggressive biological behavior of these tumors parallels those TNBCs in people (Nguyen et al. 2018).

The current standard of care for treatment of mammary carcinoma in people involves some combination of surgery, radiation therapy, chemotherapy, hormone therapy, and targeted therapy (Dhankhar et al. 2010). Surgery typically involves a unilateral or bilateral mastectomy, which is invasive and frequently associated with cosmetic deformities. Radiation therapy may cause decreased sensation to the areas as well as moderate to severe skin irritation characterized by erythema, moist desquamation, and subsequent pruritus (Akram and Siddiqui 2012; Nounou et al. 2015). Hormone therapies, such as GnRH agonists, ER antagonists (tamoxifen), and aromatase inhibitors, are typically reserved for patients with tumors that express ER and/or PR, and significantly prolongs survival in these patients. Although the severity of side effects associated with these therapies is less than those caused by chemotherapy, common side effects include hot flashes, fatigue, gastrointestinal upset, weight gain, and severe mood swings characterized by depression and anxiety, which can be debilitating. Additionally, long-term treatment has been associated with osteoporosis, putting patients at risk for bone fracture and/or chronic pain (Burstein and Griggs 2010).

Chemotherapy remains the treatment of choice for TNBC. Chemotherapy protocols using some combination of anthracyclines and taxanes decrease the risk of cancer-related death by about 33% (Early Breast Cancer Trialists' Collaborative Group et al. 2012). Most chemotherapy protocols are administered over multiple weeks and are frequently associated with debilitating side effects, such as cardiotoxicity (anthracyclines), hair loss, nausea, and severe bone marrow suppression with subsequent sepsis, among others (Valero 1997). HER2-directed therapy (Trastuzumab, Herceptin) has recently become the standard of care for patients with HER2+ breast cancer as it decreases the risk of disease reoccurrence by about 50% compared to chemotherapy alone (Callahan and Hurvitz 2011; Swain et al. 2014). Although direct therapies appear to be less debilitating, flu-like symptoms and cardiotoxicity occur with relative frequency (Ewer and Ewer 2008).

Regardless of treatment, early detection is the key to achieving remission and long-term survival. Approximately 20–30% of women diagnosed during the early stages of disease will develop distant metastasis. Despite aggressive treatment with current standard of care therapy, historically the median survival time for patients with stage 4 breast cancer was 3 years, with only 22% of patients living 5 years (Selzner et al. 2000). Development of novel targeted therapies is ongoing and results are promising with significant improvements in survival times, however, the prognosis remains grim for those patients who are not good candidates for such therapies, such as TNBC patients. Thus, ablative techniques, like IRE, have become an

attractive treatment option for these patients, as efficacy is not dependent on hormone receptor expression. Additionally, electric fields >600 V/cm applied to TNBC cells appear capable of downregulating thymic stromal lymphopoietin (TSLP) signaling, a promoter of the pro-cancer phenotype. This results in an antitumor immune response capable of transforming a "pro-cancer" microenvironment into one that is "anti-cancer." Given the predominance of TNBC in veterinary patients and the limited availability (due to accessibility and cost) of recently developed directed therapies, IRE offers a new and alternative treatment option that may be capable of improving long-term outcomes in these patients as well (Goswami et al. 2017).

Traditional breast cancer ablative techniques, such as radiofrequency ablation and high-intensity focused ultrasound (HIFU) have been associated with damage to the skin overlying breast tissue, particularly in patients with large and/or superficial tumors (Li et al. 2016; Palussiere et al. 2012). The feasibility and safety of IRE treatment of breast tissue have been demonstrated using animal models (Zhang et al. 2017; Li et al. 2016). Cutaneous effects, and gross and histopathologic changes associated with IRE delivery to breast tissue have been evaluated in a porcine model where the untreated contralateral breast tissue served as controls (Li et al. 2016). Transient changes in skin color were observed, corresponding with the skin-electrode distance and absent at distances greater than 5 mm. A rabbit orthotopic breast cancer model was also used to characterize IRE-induced skin damage and subsequent repair. IRE was able to successfully ablate all targeted breast tissue or tumor followed by complete regeneration of mammary tissue and overlying skin in the absence of fibrosis or mass formation (Li et al. 2016). Pectoralis muscle injury, despite skin preservation following IRE delivery to breast tissue, was reported in a safety and feasibility study utilizing normal rabbit models. Histologic lesions were similar to those described previously with regards to the presence of necrosis and apoptosis and preservation of critical interstitial components, but contained marked fibrous and granulation tissue following repair (Zhang et al. 2017). Results of these preliminary studies suggest IRE provides a treatment option for breast cancer that maintains esthetics.

IRE has been shown to effectively ablate local tumors regardless of hormone receptor expression, resulting in an immunologic cell death that provides the unique benefit of promoting systemic antitumor immunity capable of targeting distant lesions. This response was demonstrated in a study evaluating high-frequency irreversible electroporation (H-FIRE) in an orthotopic mouse 4T1 mammary model (Ringel-Scaia et al. 2019). H-FIRE delivery consisted of 200 bursts of bipolar PEFs at a frequency of 1 burst per second for an energized time of 100 μs per burst using a (2-5-2 μs) burst scheme. H-FIRE delivery resulted in local tumor ablation and shifted the tumor microenvironment to a pro-inflammatory state. Additionally, a significant decrease in the number of circulating metastatic cells was observed in mice that had their mammary tumors treated with H-FIRE compared to untreated mice. 4T1 cells were treated in vitro with H-FIRE or cryoablation and the resulting cell-free supernatant was injected IV into mice 10 days prior to injecting cancer cells into a mammary fat pad. Mice that received lysates from cells treated with H-FIRE

demonstrated a significant decrease in tumor size compared to both the cryoablation lysate and the control groups. Mice treated with either cryoablation lysate or H-FIRE lysate also demonstrated a significant decrease in circulating metastatic cancer cells compared to control groups. Results of this study suggest that H-FIRE activates the local innate immune system and generates neoantigens from cancer cells in their native form capable of stimulating the adaptive immune system and attenuating mammary tumor progression (Ringel-Scaia et al. 2019).

6 Summary

Irreversible electroporation applications in veterinary medicine have been limited to clinical trials evaluating the safety and feasibility of this technology for the treatment of solid tumors that are not otherwise amenable to standard of care therapy. The nonthermal ablation induced by IRE results in a more predictable ablation volume compared to thermal ablation techniques, further reducing damage to adjacent critical structures. Additionally, tumor neoantigens released following IRE remain in their native form, unaltered by temperature, and appear capable of inducing a robust systemic antitumor immune response, essentially serving as an "in-situ" vaccine. The recent development of next-generation IRE, H-FIRE, has further improved treatment precision and feasibility by overcoming some important limitations of IRE, such as treatment-induced muscle tetany and cardiac asynchrony. Patient-specific pre-treatment planning using numerical models based on CT images to predict electric field distribution throughout the target lesion has greatly enhanced the precision and efficacy of IRE ablation. Furthermore, the development of minimally invasive delivery techniques makes IRE even more attractive for treatment of solid tumors that would otherwise require highly invasive therapies. Companion animals with naturally occurring cancers continue to serve as large animal models for further investigation into the safety and efficacy of various IRE applications, including ablation of superficial and deep-seated tumors as well as blood–brain barrier disruption to enhance drug delivery to brain tumors. Clinical trials investigating the application of H-FIRE for treatment of canine pancreatic and lung tumors are currently ongoing. Results of these clinical trials will be imperative prior to translating this technology into human clinical trials. Future veterinary studies should aim to define the size threshold for effective treatment, as large tumors remain a significant challenge despite advancements in IRE delivery.

References

Ahmed M, Brace CL, Lee FT Jr, Goldberg SN (2011) Principles of and advances in percutaneous ablation. Radiology 258(2):351–369. https://doi.org/10.1148/radiol.10081634

Akram M, Siddiqui SA (2012) Breast cancer management: past, present and evolving. Indian J Cancer 49(3):277–282. https://doi.org/10.4103/0019-509X.104486

Alnaggar M, Qaid AM, Chen J, Niu L, Xu K (2018) Irreversible electroporation of malignant liver tumors: effect on laboratory values. Oncol Lett 16(3):3881–3888. https://doi.org/10.3892/ol.2018.9058

Ansari D, Kristoffersson S, Andersson R, Bergenfeldt M (2017) The role of irreversible electroporation (IRE) for locally advanced pancreatic cancer: a systematic review of safety and efficacy. Scand J Gastroenterol 52(11):1165–1171. https://doi.org/10.1080/00365521.2017.1346705

Appelbaum L, Ben-David E, Sosna J, Nissenbaum Y, Goldberg SN (2012) US findings after irreversible electroporation ablation: radiologic-pathologic correlation. Radiology 262 (1):117–125. https://doi.org/10.1148/radiol.11110475

Appelbaum L, Ben-David E, Faroja M, Nissenbaum Y, Sosna J, Goldberg SN (2014) Irreversible electroporation ablation: creation of large-volume ablation zones in in vivo porcine liver with four-electrode arrays. Radiology 270(2):416–424. https://doi.org/10.1148/radiol.13130349

Arena CB, Sano MB, Rossmeisl JH Jr, Caldwell JL, Garcia PA, Rylander MN, Davalos RV (2011a) High-frequency irreversible electroporation (H-FIRE) for non-thermal ablation without muscle contraction. Biomed Eng Online 10:102. https://doi.org/10.1186/1475-925X-10-102

Arena CB, Sano MB, Rylander MN, Davalos RV (2011b) Theoretical considerations of tissue electroporation with high-frequency bipolar pulses. IEEE Trans Biomed Eng 58(5):1474–1482. https://doi.org/10.1109/TBME.2010.2102021

Arena CB, Szot CS, Garcia PA, Rylander MN, Davalos RV (2012) A three-dimensional in vitro tumor platform for modeling therapeutic irreversible electroporation. Biophys J 103 (9):2033–2042. https://doi.org/10.1016/j.bpj.2012.09.017

Au JT, Wong J, Mittra A, Carpenter S, Haddad D, Carson J, Jayaraman S, Monette S, Solomon SB, Ezell P, Fong Y (2011) Irreversible electroporation is a surgical ablation technique that enhances gene transfer. Surgery 150(3):474–479. https://doi.org/10.1016/j.surg.2011.07.007

Aupperle-Lellbach H, Torner K, Staudacher M, Muller E, Steiger K, Klopfleisch R (2019) Characterization of 22 Canine pancreatic carcinomas and review of literature. J Comp Pathol 173:71–82. https://doi.org/10.1016/j.jcpa.2019.10.008

Ball C, Thomson KR, Kavnoudias H (2010) Irreversible electroporation: a new challenge in "out of operating theater" anesthesia. Anesth Analg 110(5):1305–1309. https://doi.org/10.1213/ANE.0b013e3181d27b30

Balogh J, Victor D 3rd, Asham EH, Burroughs SG, Boktour M, Saharia A, Li X, Ghobrial RM, Monsour HP Jr (2016) Hepatocellular carcinoma: a review. J Hepatocell Carcinoma 3:41–53. https://doi.org/10.2147/JHC.S61146

Beitel-White N, Bhonsle S, Martin RCG, Davalos RV (2018) Electrical characterization of human biological tissue for irreversible electroporation treatments. Conf Proc IEEE Eng Med Biol Soc 2018:4170–4173. https://doi.org/10.1109/EMBC.2018.8513341

Ben-David E, Appelbaum L, Sosna J, Nissenbaum I, Goldberg SN (2012) Characterization of irreversible electroporation ablation in in vivo porcine liver. AJR Am J Roentgenol 198(1): W62–W68. https://doi.org/10.2214/AJR.11.6940

Ben-David E, Ahmed M, Faroja M, Moussa M, Wandel A, Sosna J, Appelbaum L, Nissenbaum I, Goldberg SN (2013) Irreversible electroporation: treatment effect is susceptible to local environment and tissue properties. Radiology 269(3):738–747. https://doi.org/10.1148/radiol.13122590

Bhonsle S, Arena C, Sweeney D, Davalos R (2015) Mitigation of impedance changes due to electroporation therapy using bursts of high-frequency bipolar pulses. Biomed Eng Online 14 (3):S3. https://doi.org/10.1186/1475-925X-14-S3-S3

Bhonsle S, Bonakdar M, Neal RE 2nd, Aardema C, Robertson JL, Howarth J, Kavnoudias H, Thomson KR, Goldberg SN, Davalos RV (2016) Characterization of irreversible electroporation ablation with a validated perfused organ model. J Vasc Interv Radiol 27(12):1913–1922. https://doi.org/10.1016/j.jvir.2016.07.012

Bhonsle S, Lorenzo MF, Safaai-Jazi A, Davalos RV (2018) Characterization of nonlinearity and dispersion in tissue impedance during high-frequency electroporation. IEEE Trans Biomed Eng 65(10):2190–2201. https://doi.org/10.1109/TBME.2017.2787038

Bhutiani N, Philips P, Scoggins CR, McMasters KM, Potts MH, Martin RC (2016) Evaluation of tolerability and efficacy of irreversible electroporation (IRE) in treatment of Child-Pugh B (7/8) hepatocellular carcinoma (HCC). HPB (Oxford) 18(7):593–599. https://doi.org/10.1016/j.hpb.2016.03.609

Bianchini G, Balko JM, Mayer IA, Sanders ME, Gianni L (2016) Triple-negative breast cancer: challenges and opportunities of a heterogeneous disease. Nat Rev Clin Oncol 13(11):674–690. https://doi.org/10.1038/nrclinonc.2016.66

Bill-Axelson A, Holmberg L, Garmo H, Taari K, Busch C, Nordling S, Haggman M, Andersson SO, Andren O, Steineck G, Adami HO, Johansson JE (2018) Radical prostatectomy or watchful waiting in prostate cancer - 29-year follow-up. N Engl J Med 379(24):2319–2329. https://doi.org/10.1056/NEJMoa1807801

Bonakdar M, Latouche EL, Mahajan RL, Davalos RV (2015) The feasibility of a smart surgical probe for verification of ire treatments using electrical impedance spectroscopy. IEEE Trans Biomed Eng 62(11):2674–2684. https://doi.org/10.1109/TBME.2015.2441636

Bower M, Sherwood L, Li Y, Martin R (2011) Irreversible electroporation of the pancreas: definitive local therapy without systemic effects. J Surg Oncol 104(1):22–28. https://doi.org/10.1002/jso.21899

Brock R, White N, Ringel-Scaia V, Coutermarsh-Ott S, Eden K, Coutri J, Manuchehrabadi N, Davalos R, Allen I (2019) Irreversible electroporation stimulates a pro-inflammatory tumor microenvironment in pancreatic cancer. J Immunol 202(1):194

Burstein HJ, Griggs JJ (2010) Adjuvant hormonal therapy for early-stage breast cancer. Surg Oncol Clin N Am 19(3):639–647. https://doi.org/10.1016/j.soc.2010.03.006

Byron CR, DeWitt MR, Latouche EL, Davalos RV, Robertson JL (2019) Treatment of infiltrative superficial tumors in awake standing horses using novel high-frequency pulsed electrical fields. Front Vet Sci 6:265. https://doi.org/10.3389/fvets.2019.00265

Callahan R, Hurvitz S (2011) Human epidermal growth factor receptor-2-positive breast cancer: current management of early, advanced, and recurrent disease. Curr Opin Obstet Gynecol 23(1):37–43. https://doi.org/10.1097/gco.0b013e3283414e87

Callery MP, Chang KJ, Fishman EK, Talamonti MS, William Traverso L, Linehan DC (2009) Pretreatment assessment of resectable and borderline resectable pancreatic cancer: expert consensus statement. Ann Surg Oncol 16(7):1727–1733. https://doi.org/10.1245/s10434-009-0408-6

Campelo S, Valerio M, Ahmed HU, Hu Y, Arena SL, Neal RE 2nd, Emberton M, Arena CB (2017) An evaluation of irreversible electroporation thresholds in human prostate cancer and potential correlations to physiological measurements. APL Bioeng 1(1):016101. https://doi.org/10.1063/1.5005828

Cannon R, Ellis S, Hayes D, Narayanan G, Martin RC 2nd (2013) Safety and early efficacy of irreversible electroporation for hepatic tumors in proximity to vital structures. J Surg Oncol 107(5):544–549. https://doi.org/10.1002/jso.23280

Charpentier KP, Wolf F, Noble L, Winn B, Resnick M, Dupuy DE (2010) Irreversible electroporation of the pancreas in swine: a pilot study. HPB (Oxford) 12(5):348–351. https://doi.org/10.1111/j.1477-2574.2010.00174.x

Charpentier KP, Wolf F, Noble L, Winn B, Resnick M, Dupuy DE (2011) Irreversible electroporation of the liver and liver hilum in swine. HPB (Oxford) 13(3):168–173. https://doi.org/10.1111/j.1477-2574.2010.00261.x

Chen Z, Hambardzumyan D (2018) Immune microenvironment in glioblastoma subtypes. Front Immunol 9:1004. https://doi.org/10.3389/fimmu.2018.01004

Chua TC, Saxena A (2010) Extended pancreaticoduodenectomy with vascular resection for pancreatic cancer: a systematic review. J Gastrointest Surg 14(9):1442–1452. https://doi.org/10.1007/s11605-009-1129-7

Cindric H, Kos B, Tedesco G, Cadossi M, Gasbarrini A, Miklavcic D (2018) Electrochemotherapy of spinal metastases using transpedicular approach: a numerical feasibility study. Technol Cancer Res Treat 17:1533034618770253. https://doi.org/10.1177/1533034618770253

Clark C (2017) Safety of next generation high frequency irreversible electroporation (H-FIRE) in a porcine pancreatic cancer treatment model. HPB. https://doi.org/10.1016/j.hpb.2017.02.366

Collettini F, Enders J, Stephan C, Fischer T, Baur ADJ, Penzkofer T, Busch J, Hamm B, Gebauer B (2019) Image-guided irreversible electroporation of localized prostate cancer: functional and oncologic outcomes. Radiology 292(1):250–257. https://doi.org/10.1148/radiol.2019181987

Corovic S, Mir LM, Miklavcic D (2012) In vivo muscle electroporation threshold determination: realistic numerical models and in vivo experiments. J Membr Biol 245(9):509–520. https://doi.org/10.1007/s00232-012-9432-8

Davalos RV, Otten DM, Mir LM, Rubinsky B (2004) Electrical impedance tomography for imaging tissue electroporation. IEEE Trans Biomed Eng 51(5):761–767. https://doi.org/10.1109/TBME.2004.824148

Davalos RV, Bhonsle S, Neal RE 2nd (2015) Implications and considerations of thermal effects when applying irreversible electroporation tissue ablation therapy. Prostate 75(10):1114–1118. https://doi.org/10.1002/pros.22986

DeBruin KA, Krassowska W (1999) Modeling electroporation in a single cell. II. Effects of ionic concentrations. Biophys J 77(3):1225–1233. https://doi.org/10.1016/S0006-3495(99)76974-2

Deodhar A, Dickfeld T, Single GW, Hamilton WC Jr, Thornton RH, Sofocleous CT, Maybody M, Gonen M, Rubinsky B, Solomon SB (2011) Irreversible electroporation near the heart: ventricular arrhythmias can be prevented with ECG synchronization. AJR Am J Roentgenol 196(3):W330–W335. https://doi.org/10.2214/AJR.10.4490

Dettin M, Sieni E, Zamuner A, Marino R, Sgarbossa P, Lucibello M, Tosi AL, Keller F, Campana LG, Signori E (2019) A novel 3D Scaffold for cell growth to assess electroporation efficacy. Cells 8(11). https://doi.org/10.3390/cells8111470

Dhankhar R, Vyas SP, Jain AK, Arora S, Rath G, Goyal AK (2010) Advances in novel drug delivery strategies for breast cancer therapy. Artif Cells Blood Substit Immobil Biotechnol 38(5):230–249. https://doi.org/10.3109/10731199.2010.494578

Dollinger M, Beyer LP, Haimerl M, Niessen C, Jung EM, Zeman F, Stroszczynski C, Wiggermann P (2015) Adverse effects of irreversible electroporation of malignant liver tumors under CT fluoroscopic guidance: a single-center experience. Diagn Interv Radiol 21(6):471–475. https://doi.org/10.5152/dir.2015.14442

Dunki-Jacobs EM, Philips P, Martin RC 2nd (2014) Evaluation of resistance as a measure of successful tumor ablation during irreversible electroporation of the pancreas. J Am Coll Surg 218(2):179–187. https://doi.org/10.1016/j.jamcollsurg.2013.10.013

Early Breast Cancer Trialists' Collaborative Group, Peto R, Davies C, Godwin J, Gray R, Pan HC, Clarke M, Cutter D, Darby S, McGale P, Taylor C, Wang YC, Bergh J, Di Leo A, Albain K, Swain S, Piccart M, Pritchard K (2012) Comparisons between different polychemotherapy regimens for early breast cancer: meta-analyses of long-term outcome among 100,000 women in 123 randomised trials. Lancet 379(9814):432–444. https://doi.org/10.1016/S0140-6736(11)61625-5

Edd JF, Davalos RV (2007) Mathematical modeling of irreversible electroporation for treatment planning. Technol Cancer Res Treat 6(4):275–286. https://doi.org/10.1177/153303460700600403

Elgenedy MA et al (2017) A transition arm modular multilevel universal pulse-waveform generator for electroporation applications. IEEE Trans Power Electronics 32(12):8979–8991

Ellis TL, Garcia PA, Rossmeisl JH Jr, Henao-Guerrero N, Robertson J, Davalos RV (2011) Nonthermal irreversible electroporation for intracranial surgical applications. Laboratory investigation. J Neurosurg 114(3):681–688. https://doi.org/10.3171/2010.5.JNS091448

Ewer SM, Ewer MS (2008) Cardiotoxicity profile of trastuzumab. Drug Saf 31(6):459–467. https://doi.org/10.2165/00002018-200831060-00002

Ford MS, Young KJ, Zhang Z, Ohashi PS, Zhang L (2002) The immune regulatory function of lymphoproliferative double negative T cells in vitro and in vivo. J Exp Med 196(2):261–267

Fritz S, Sommer CM, Vollherbst D, Wachter MF, Longerich T, Sachsenmeier M, Knapp J, Radeleff BA, Werner J (2015) Irreversible electroporation of the pancreas is feasible and safe in a porcine survival model. Pancreas 44(5):791–798. https://doi.org/10.1097/MPA.0000000000000331

Fruhling P, Nilsson A, Duraj F, Haglund U, Noren A (2017) Single-center nonrandomized clinical trial to assess the safety and efficacy of irreversible electroporation (IRE) ablation of liver tumors in humans: short to mid-term results. Eur J Surg Oncol 43(4):751–757. https://doi.org/10.1016/j.ejso.2016.12.004

Garcia PA, Rossmeisl JH Jr, Neal RE 2nd, Ellis TL, Olson JD, Henao-Guerrero N, Robertson J, Davalos RV (2010) Intracranial nonthermal irreversible electroporation: in vivo analysis. J Membr Biol 236(1):127–136. https://doi.org/10.1007/s00232-010-9284-z

Garcia PA, Rossmeisl JH Jr, Robertson JL, Olson JD, Johnson AJ, Ellis TL, Davalos RV (2012) 7.0-T magnetic resonance imaging characterization of acute blood-brain-barrier disruption achieved with intracranial irreversible electroporation. PLoS One 7(11):e50482. https://doi.org/10.1371/journal.pone.0050482

Garcia PA, Kos B, Rossmeisl JH Jr, Pavliha D, Miklavcic D, Davalos RV (2017) Predictive therapeutic planning for irreversible electroporation treatment of spontaneous malignant glioma. Med Phys 44(9):4968–4980. https://doi.org/10.1002/mp.12401

Gehl J, Mir LM (1999) Determination of optimal parameters for in vivo gene transfer by electroporation, using a rapid in vivo test for cell permeabilization. Biochem Biophys Res Commun 261 (2):377–380. https://doi.org/10.1006/bbrc.1999.1014

Golberg A, Bruinsma BG, Uygun BE, Yarmush ML (2015) Tissue heterogeneity in structure and conductivity contribute to cell survival during irreversible electroporation ablation by "electric field sinks". Sci Rep 5:8485. https://doi.org/10.1038/srep08485

Goswami I, Coutermarsh-Ott S, Morrison RG, Allen IC, Davalos RV, Verbridge SS, Bickford LR (2017) Irreversible electroporation inhibits pro-cancer inflammatory signaling in triple negative breast cancer cells. Bioelectrochemistry 113:42–50. https://doi.org/10.1016/j.bioelechem.2016.09.003

Guenther E, Klein N, Zapf S, Weil S, Schlosser C, Rubinsky B, Stehling MK (2019) Prostate cancer treatment with Irreversible Electroporation (IRE): safety, efficacy and clinical experience in 471 treatments. PLoS One 14(4):e0215093. https://doi.org/10.1371/journal.pone.0215093

Guo Y, Zhang Y, Nijm GM, Sahakian AV, Yang GY, Omary RA, Larson AC (2011) Irreversible electroporation in the liver: contrast-enhanced inversion-recovery MR imaging approaches to differentiate reversibly electroporated penumbra from irreversibly electroporated ablation zones. Radiology 258(2):461–468. https://doi.org/10.1148/radiol.10100645

Han Y (2019) Safety and feasibility of prostatic tissue ablation in dogs by percutaneous irreversible electroporation (IRE) using a newly developed high-voltage steep-pulse-therapy device. Int J Clin Exp Med 12(7):8014–8023

Ivey JW, Wasson EM, Alinezhadbalalami N, Kanitkar A, Debinski W, Sheng Z, Davalos RV, Verbridge SS (2019) Characterization of ablation thresholds for 3D-cultured patient-derived glioma stem cells in response to high-frequency irreversible electroporation. Research (Wash D C). https://doi.org/10.34133/2019/8081315

Ivorra A, Al-Sakere B, Rubinsky B, Mir LM (2009) In vivo electrical conductivity measurements during and after tumor electroporation: conductivity changes reflect the treatment outcome. Phys Med Biol 54(19):5949–5963. https://doi.org/10.1088/0031-9155/54/19/019

Kalra N, Gupta P, Gorsi U, Bhujade H, Chaluvashetty SB, Duseja A, Singh V, Dhiman RK, Chawla YK, Khandelwal N (2019) Irreversible electroporation for unresectable hepatocellular carcinoma: initial experience. Cardiovasc Intervent Radiol 42(4):584–590. https://doi.org/10.1007/s00270-019-02164-2

Kane GMO, Knox JJ (2018) Locally advanced pancreatic cancer: an emerging entity. Curr Probl Cancer 42(1):12–25. https://doi.org/10.1016/j.currproblcancer.2017.10.006

Kato H, Usui M, Isaji S, Nagakawa T, Wada K, Unno M, Nakao A, Miyakawa S, Ohta T (2013) Clinical features and treatment outcome of borderline resectable pancreatic head/body cancer: a

multi-institutional survey by the Japanese Society of Pancreatic Surgery. J Hepatobiliary Pancreat Sci 20(6):601–610. https://doi.org/10.1007/s00534-013-0595-1

Kingham TP, Karkar AM, D'Angelica MI, Allen PJ, Dematteo RP, Getrajdman GI, Sofocleous CT, Solomon SB, Jarnagin WR, Fong Y (2012) Ablation of perivascular hepatic malignant tumors with irreversible electroporation. J Am Coll Surg 215(3):379–387. https://doi.org/10.1016/j.jamcollsurg.2012.04.029

Kinsey JR, Gilson SD, Hauptman J, Mehler SJ, May LR (2015) Factors associated with long-term survival in dogs undergoing liver lobectomy as treatment for liver tumors. Can Vet J 56 (6):598–604

Kos B, Voigt P, Miklavcic D, Moche M (2015) Careful treatment planning enables safe ablation of liver tumors adjacent to major blood vessels by percutaneous irreversible electroporation (IRE). Radiol Oncol 49(3):234–241. https://doi.org/10.1515/raon-2015-0031

Kranjc M, Kranjc S, Bajd F, Sersa G, Sersa I, Miklavcic D (2017) Predicting irreversible electroporation-induced tissue damage by means of magnetic resonance electrical impedance tomography. Sci Rep 7(1):10323. https://doi.org/10.1038/s41598-017-10846-5

Kwon D, McFarland K, Velanovich V, Martin RC (2014) Borderline and locally advanced pancreatic adenocarcinoma margin accentuation with intraoperative irreversible electroporation. Surgery 156(4):910–922. https://doi.org/10.1016/j.surg.2014.06.058

Langan RC, Goldman DA, D'Angelica MI, DeMatteo RP, Allen PJ, Balachandran VP, Jarnagin WR, Kingham TP (2017) Recurrence patterns following irreversible electroporation for hepatic malignancies. J Surg Oncol 115(6):704–710. https://doi.org/10.1002/jso.24570

Latouche EL, Sano MB, Lorenzo MF, Davalos RV, Martin RCG 2nd (2017) Irreversible electroporation for the ablation of pancreatic malignancies: a patient-specific methodology. J Surg Oncol 115(6):711–717. https://doi.org/10.1002/jso.24566

Latouche EL, Arena CB, Ivey JW, Garcia PA, Pancotto TE, Pavlisko N, Verbridge SS, Davalos RV, Rossmeisl JH (2018) High-frequency irreversible electroporation for intracranial meningioma: a feasibility study in a spontaneous canine tumor model. Technol Cancer Res Treat 17:1533033818785285. https://doi.org/10.1177/1533033818785285

Lee YJ, Lu DS, Osuagwu F, Lassman C (2012) Irreversible electroporation in porcine liver: short- and long-term effect on the hepatic veins and adjacent tissue by CT with pathological correlation. Invest Radiol 47(11):671–675. https://doi.org/10.1097/RLI.0b013e318274b0df

Leroy BE, Northrup N (2009) Prostate cancer in dogs: comparative and clinical aspects. Vet J 180 (2):149–162. https://doi.org/10.1016/j.tvjl.2008.07.012

Li S, Chen F, Shen L, Zeng Q, Wu P (2016) Percutaneous irreversible electroporation for breast tissue and breast cancer: safety, feasibility, skin effects and radiologic-pathologic correlation in an animal study. J Transl Med 14(1):238. https://doi.org/10.1186/s12967-016-0993-7

Lim M, Xia Y, Bettegowda C, Weller M (2018) Current state of immunotherapy for glioblastoma. Nat Rev Clin Oncol 15(7):422–442. https://doi.org/10.1038/s41571-018-0003-5

Linecker M, Pfammatter T, Kambakamba P, DeOliveira ML (2016) Ablation strategies for locally advanced pancreatic cancer. Dig Surg 33(4):351–359. https://doi.org/10.1159/000445021

Liptak JM, Dernell WS, Monnet E, Powers BE, Bachand AM, Kenney JG, Withrow SJ (2004) Massive hepatocellular carcinoma in dogs: 48 cases (1992-2002). J Am Vet Med Assoc 225 (8):1225–1230

Liu Y, Xiong Z, Zhou W, Hua Y, Li C, Yao C (2012) Percutaneous ultrasound-guided irreversible electroporation: a goat liver study. Oncol Lett 4(3):450–454. https://doi.org/10.3892/ol.2012.781

Lorenzo MF, Thomas SC, Kani Y, Hinckley J, Lee M, Adler J, Verbridge SS, Hsu FC, Robertson JL, Davalos RV, Rossmeisl JH Jr (2019) Temporal characterization of blood-brain barrier disruption with high-frequency electroporation. Cancers (Basel) 11(12). https://doi.org/10.3390/cancers11121850

Lorenzo MF, Bhonsle S, Arena CB, Davalos RV (2020) Rapid impedance spectroscopy for monitoring tissue impedance, temperature, and treatment outcome during electroporation-based therapies. IEEE Trans Biomed Eng. https://doi.org/10.1109/TBME.2020.3036535

Mafeld S, Wong JJ, Kibriya N, Stenberg B, Manas D, Bassett P, Aslam T, Evans J, Littler P (2019) Percutaneous irreversible electroporation (IRE) of hepatic malignancy: a bi-institutional analysis of safety and outcomes. Cardiovasc Intervent Radiol 42(4):577–583. https://doi.org/10.1007/s00270-018-2120-z

Martin RC, McFarland K, Ellis S, Velanovich V (2013) Irreversible electroporation in locally advanced pancreatic cancer: potential improved overall survival. Ann Surg Oncol 20(3):S443–S449. https://doi.org/10.1245/s10434-012-2736-1

Martina MN, Noel S, Saxena A, Rabb H, Hamad AR (2015) Double negative (DN) alphabeta T cells: misperception and overdue recognition. Immunol Cell Biol 93(3):305–310. https://doi.org/10.1038/icb.2014.99

Mercadal B, Arena CB, Davalos RV, Ivorra A (2017) Avoiding nerve stimulation in irreversible electroporation: a numerical modeling study. Phys Med Biol 62(20):8060–8079. https://doi.org/10.1088/1361-6560/aa8c53

Miklavcic D, Semrov D, Mekid H, Mir LM (2000) A validated model of in vivo electric field distribution in tissues for electrochemotherapy and for DNA electrotransfer for gene therapy. Biochim Biophys Acta 1523(1):73–83. https://doi.org/10.1016/s0304-4165(00)00101-x

Miklavcic D, Sel D, Cukjati D, Batiuskaite D, Slivnik T, Mir L (2004) Sequential finite element model of tissue electropermeabilisation. Conf Proc IEEE Eng Med Biol Soc 2004:3551–3554. https://doi.org/10.1109/IEMBS.2004.1403998

Miklavcic D, Pucihar G, Pavlovec M, Ribaric S, Mali M, Macek-Lebar A, Petkovsek M, Nastran J, Kranic S, Cemazar M, Sersa G (2005) The effect of high frequency electric pulses on muscle contractions and anti-tumor efficiency in vivo for a potential use in clinical electrochemotherapy. Bioelectrochemistry 65(2):121–128. https://doi.org/10.1016/j.bioelechem.2004.07.004

Miklavcic D, Mali B, Kos B, Heller R, Sersa G (2014) Electrochemotherapy: from the drawing board into medical practice. Biomed Eng Online 13(1):29. https://doi.org/10.1186/1475-925X-13-29

Miller L, Leor J, Rubinsky B (2005) Cancer cells ablation with irreversible electroporation. Technol Cancer Res Treat 4(6):699–705. https://doi.org/10.1177/153303460500400615

Narayanan G (2015) Irreversible electroporation. Semin Intervent Radiol 32(4):349–355. https://doi.org/10.1055/s-0035-1564706

Narayanan G, Hosein P, Arora G, Barbery K, Froud T, Livingstone A, Franceschi D, Rocha Lime CM, Yrizarry J (2012) Percutaneous irreversible electroporation for downstaging and control of unresectable pancreatic adenocarcinoma. J Vasc Interven Radiol 23(12):1613–1612. https://doi.org/10.1016/j.jvir.2012.09.012

Narayanan G, Bhatia S, Echenique A, Suthar R, Barbery K, Yrizarry J (2014) Vessel patency post irreversible electroporation. Cardiovasc Intervent Radiol 37(6):1523–1529. https://doi.org/10.1007/s00270-014-0988-9

Neal RE, Singh R, Hatcher HC, Kock ND, Torti SV, Davalos RV (2010a) Treatment of breast cancer through the application of irreversible electroporation using a novel minimally invasive single needle electrode. Breast Cancer Res Treat 123(1):295–301. https://doi.org/10.1007/s10549-010-0803-5

Neal RE, Garcia PA, Rossmeisl JH, Davalos RV (2010b) A study using irreversible electroporation to treat large, irregular tumors in a canine patient. Conf Proc IEEE Eng Med Biol Soc 2010:2747–2750. https://doi.org/10.1109/IEMBS.2010.5626372

Neal RE, Garcia PA, Robertson JL, Davalos RV (2012) Experimental characterization and numerical modeling of tissue electrical conductivity during pulsed electric fields for irreversible electroporation treatment planning. IEEE Trans Biomed Eng 59(4):1076–1085. https://doi.org/10.1109/TBME.2012.2182994

Neal RE, Millar JL, Kavnoudias H, Royce P, Rosenfeldt F, Pham A, Smith R, Davalos RV, Thomson KR (2014) In vivo characterization and numerical simulation of prostate properties for non-thermal irreversible electroporation ablation. Prostate 74(5):458–468. https://doi.org/10.1002/pros.22760

Neal RE, Garcia PA, Kavnoudias H, Rosenfeldt F, McLean CA, Earl V, Bergman J, Davalos RV, Thomson KR (2015) In vivo irreversible electroporation kidney ablation: experimentally correlated numerical models. IEEE Trans Biomed Eng 62(2):561–569. https://doi.org/10.1109/TBME.2014.2360374

Nguyen F, Pena L, Ibisch C, Loussouarn D, Gama A, Rieder N, Belousov A, Campone M, Abadie J (2018) Canine invasive mammary carcinomas as models of human breast cancer. Part 1: natural history and prognostic factors. Breast Cancer Res Treat 167(3):635–648. https://doi.org/10.1007/s10549-017-4548-2

Niessen C, Beyer LP, Pregler B, Dollinger M, Trabold B, Schlitt HJ, Jung EM, Stroszczynski C, Wiggermann P (2016) Percutaneous ablation of hepatic tumors using irreversible electroporation: a prospective safety and midterm efficacy study in 34 patients. J Vasc Interv Radiol 27(4):480–486. https://doi.org/10.1016/j.jvir.2015.12.025

Niessen C, Thumann S, Beyer L, Pregler B, Kramer J, Lang S, Teufel A, Jung EM, Stroszczynski C, Wiggermann P (2017) Percutaneous irreversible electroporation: long-term survival analysis of 71 patients with inoperable malignant hepatic tumors. Sci Rep 7:43687. https://doi.org/10.1038/srep43687

Nounou MI, ElAmrawy F, Ahmed N, Abdelraouf K, Goda S, Syed-Sha-Qhattal H (2015) Breast cancer: conventional diagnosis and treatment modalities and recent patents and technologies. Breast Cancer (Auckl) 9(Suppl 2):17–34. https://doi.org/10.4137/BCBCR.S29420

O'Brien TJ, Passeri M, Lorenzo MF, Sulzer JK, Lyman WB, Swet JH, Vrochides D, Baker EH, Iannitti DA, Davalos RV, McKillop IH (2019) Experimental high-frequency irreversible electroporation using a single-needle delivery approach for nonthermal pancreatic ablation in vivo. J Vasc Interv Radiol 30(6):854–862. https://doi.org/10.1016/j.jvir.2019.01.032

Onik G, Rubinsky B (2010) Irreversible electroporation: first patient experience focal therapy of prostate cancer. In: Rubinsky B (ed) Irreversible electroporation, Series in biomedical engineering. Springer, Berlin, Heidelberg. https://doi.org/10.1007/978-3-642-05420-4_10

Onik G, Mikus P, Rubinsky B (2007) Irreversible electroporation: implications for prostate ablation. Technol Cancer Res Treat 6(4):295–300. https://doi.org/10.1177/153303460700600405

Palussiere J, Henriques C, Mauriac L, Asad-Syed M, Valentin F, Brouste V, Mathoulin-Pelissier S, Tunon de Lara C, Debled M (2012) Radiofrequency ablation as a substitute for surgery in elderly patients with nonresected breast cancer: pilot study with long-term outcomes. Radiology 264(2):597–605. https://doi.org/10.1148/radiol.12111303

Partridge BR, O'Brien TJ, Lorenzo MF, Coutermarsh-Ott SL, Barry SL, Stadler K, Muro N, Meyerhoeffer M, Allen IC, Davalos RV, Dervisis NG (2020) High-frequency irreversible electroporation for treatment of primary liver cancer: a proof-of-principle study in canine hepatocellular carcinoma. J Vasc Interv Radiol. https://doi.org/10.1016/j.jvir.2019.10.015

Pasquali S, Hadjinicolaou AV, Chiarion Sileni V, Rossi CR, Mocellin S (2018) Systemic treatments for metastatic cutaneous melanoma. Cochrane Database Syst Rev 2:CD011123. https://doi.org/10.1002/14651858.CD011123.pub2

Pavliha D, Kos B, Marcan M, Zupanic A, Sersa G, Miklavcic D (2013) Planning of electroporation-based treatments using Web-based treatment-planning software. J Membr Biol 246(11):833–842. https://doi.org/10.1007/s00232-013-9567-2

Pavlin M, Kanduser M, Rebersek M, Pucihar G, Hart FX, Magjarevic R, Miklavcic D (2005) Effect of cell electroporation on the conductivity of a cell suspension. Biophys J 88(6):4378–4390. https://doi.org/10.1529/biophysj.104.048975

Perera-Bel E, Yague C, Mercadal B, Ceresa M, Beitel-White N, Davalos R, Gonzalez B, Ivorra A (2020) EView: an electric field visualization web platform for electroporation-based therapies. Computer Methods Prog Biomed. https://doi.org/10.1016/j.cmpb.2020.105682

Pinard CJ, Hocker SE, Weishaar KM (2020) Clinical outcome in 23 dogs with exocrine pancreatic carcinoma. Vet Comp Oncol. https://doi.org/10.1111/vco.12645

Potocnik T, Miklavcic D, Lebar AM (2019) Effect of electroporation and recovery medium pH on cell membrane permeabilization, cell survival and gene transfer efficiency in vitro. Bioelectrochemistry 130. https://doi.org/10.1016/j.bioelechem.2019.107342

Priester WA (1974) Data from eleven United States and Canadian colleges of veterinary medicine on pancreatic carcinoma in domestic animals. Cancer Res 34(6):1372–1375

Pucihar G, Krmelj J, Rebersek M, Napotnik TB, Miklavcic D (2011) Equivalent pulse parameters for electroporation. IEEE Trans Biomed Eng 58(11):3279–3288. https://doi.org/10.1109/TBME.2011.2167232

Qin Z, Zeng J, Liu G, Long X, Fang G, Li Z, Xu K, Niu L (2017) Irreversible electroporation ablation of an unresectable fibrous sarcoma with 2 electrodes: a case report. Technol Cancer Res Treat. https://doi.org/10.1177/1533034617711530

Rakha EA, Reis-Filho JS, Ellis IO (2010) Combinatorial biomarker expression in breast cancer. Breast Cancer Res Treat 120(2):293–308. https://doi.org/10.1007/s10549-010-0746-x

Rawla P (2019) Epidemiology of prostate cancer. World J Oncol 10(2):63–89. https://doi.org/10.14740/wjon1191

Rebersek M, Miklavcic D (2011) Advantages and disadvantages of different concepts of electroporation pulse generation. Automatika 52(1):12–19

Redondo LM, Zahyka M, Kandratsyeu A (2019) Solid-state generation of high-frequency burst of bipolar pulses for medical applications. IEEE Trans Plasma Sci 47(8):4091–4095

Ringel-Scaia VM, Beitel-White N, Lorenzo MF, Brock RM, Huie KE, Coutermarsh-Ott S, Eden K, McDaniel DK, Verbridge SS, Rossmeisl JH Jr, Oestreich KJ, Davalos RV, Allen IC (2019) High-frequency irreversible electroporation is an effective tumor ablation strategy that induces immunologic cell death and promotes systemic anti-tumor immunity. EBioMedicine 44:112–125. https://doi.org/10.1016/j.ebiom.2019.05.036

Robinson MW, Harmon C, O'Farrelly C (2016) Liver immunology and its role in inflammation and homeostasis. Cell Mol Immunol 13(3):267–276. https://doi.org/10.1038/cmi.2016.3

Rombouts SJE, van Dijck WPM, Nijkamp MW, Derksen TC, Brosens LAA, Hoogwater FJH, van Leeuwen MS, Borel Rinkes IHM, van Hillegersberg R, Wittkampf FH, Molenaar IQ (2017) Clinical and pathological outcomes after irreversible electroporation of the pancreas using two parallel plate electrodes: a porcine model. HPB (Oxford) 19(12):1058–1065. https://doi.org/10.1016/j.hpb.2017.02.443

Rossmeisl JH, Garcia PA, Pancotto TE, Robertson JL, Henao-Guerrero N, Neal RE 2nd, Ellis TL, Davalos RV (2015) Safety and feasibility of the NanoKnife system for irreversible electroporation ablative treatment of canine spontaneous intracranial gliomas. J Neurosurg 123(4):1008–1025. https://doi.org/10.3171/2014.12.JNS141768

Rubinsky B (2007) Irreversible electroporation in medicine. Technol Cancer Res Treat 6(4):255–260. https://doi.org/10.1177/153303460700600401

Rubinsky B, Onik G, Mikus P (2007) Irreversible electroporation: a new ablation modality – clinical implications. Technol Cancer Res Treat 6(1):37–48. https://doi.org/10.1177/153303460700600106

Saini A, Breen I, Alzubaidi S, Pershad Y, Sheth R, Naidu S, Knuttinen MG, Albadawi H, Oklu R (2018) Irreversible electroporation in liver cancers and whole organ engineering. J Clin Med 8(1). https://doi.org/10.3390/jcm8010022

Scheffer HJ, Nielsen K, de Jong MC, van Tilborg AA, Vieveen JM, Bouwman AR, Meijer S, van Kuijk C, van den Tol PM, Meijerink MR (2014a) Irreversible electroporation for nonthermal tumor ablation in the clinical setting: a systematic review of safety and efficacy. J Vasc Interv Radiol 25(7):997–1011. https://doi.org/10.1016/j.jvir.2014.01.028

Scheffer HJ, Nielsen K, van Tilborg AA, Vieveen JM, Bouwman RA, Kazemier G, Niessen HW, Meijer S, van Kuijk C, van den Tol MP, Meijerink MR (2014b) Ablation of colorectal liver metastases by irreversible electroporation: results of the COLDFIRE-I ablate-and-resect study. Eur Radiol 24(10):2467–2475. https://doi.org/10.1007/s00330-014-3259-x

Scheffer HJ, Vogel JA, van den Bos W, Neal RE 2nd, van Lienden KP, Besselink MG, van Gemert MJ, van der Geld CW, Meijerink MR, Klaessens JH, Verdaasdonk RM (2016) The influence of

a metal stent on the distribution of thermal energy during irreversible electroporation. PLoS One 11(2):e0148457. https://doi.org/10.1371/journal.pone.0148457

Schmidt CR, Shires P, Mootoo M (2012) Real-time ultrasound imaging of irreversible electroporation in a porcine liver model adequately characterizes the zone of cellular necrosis. HPB (Oxford) 14(2):98–102. https://doi.org/10.1111/j.1477-2574.2011.00409.x

Selzner M, Morse MA, Vredenburgh JJ, Meyers WC, Clavien PA (2000) Liver metastases from breast cancer: long-term survival after curative resection. Surgery 127(4):383–389. https://doi.org/10.1067/msy.2000.103883

Sharabi S, Bresler Y, Ravid O, Shemesh C, Atrakchi D, Schnaider-Beeri M, Gosselet F, Dehouck L, Last D, Guez D, Daniels D, Mardor Y, Cooper I (2019) Transient blood-brain barrier disruption is induced by low pulsed electric fields in vitro: an analysis of permeability and trans-endothelial electric resistivity. Drug Deliv 26(1):459–469. https://doi.org/10.1080/10717544.2019.1571123

Sharabi S, Guez D, Daniels D, Cooper I, Atrakchi D, Liraz-Zaltsman S, Last D, Mardor Y (2020) The application of point source electroporation and chemotherapy for the treatment of glioma: a randomized controlled rat study. Sci Rep 10(1):2178. https://doi.org/10.1038/s41598-020-59152-7

Siddiqui IA, Latouche EL, DeWitt MR, Swet JH, Kirks RC, Baker EH, Iannitti DA, Vrochides D, Davalos RV, McKillop IH (2016) Induction of rapid, reproducible hepatic ablations using next-generation, high frequency irreversible electroporation (H-FIRE) in vivo. HPB (Oxford) 18(9):726–734. https://doi.org/10.1016/j.hpb.2016.06.015

Siegel RL, Miller KD, Jemal A (2017) Cancer statistics, 2017. CA Cancer J Clin 67(1):7–30. https://doi.org/10.3322/caac.21387

Silk MT, Wimmer T, Lee KS, Srimathveeravalli G, Brown KT, Kingham PT, Fong Y, Durack JC, Sofocleous CT, Solomon SB (2014) Percutaneous ablation of peribiliary tumors with irreversible electroporation. J Vasc Interv Radiol 25(1):112–118. https://doi.org/10.1016/j.jvir.2013.10.012

Stupp R, Mason WP, van den Bent MJ, Weller M, Fisher B, Taphoorn MJ, Belanger K, Brandes AA, Marosi C, Bogdahn U, Curschmann J, Janzer RC, Ludwin SK, Gorlia T, Allgeier A, Lacombe D, Cairncross JG, Eisenhauer E, Mirimanoff RO, European Organisation for Research, Treatment of Cancer Brain Tumor, Radiotherapy Groups, National Cancer Institute of Canada Clinical Trials Group (2005) Radiotherapy plus concomitant and adjuvant temozolomide for glioblastoma. N Engl J Med 352(10):987–996. https://doi.org/10.1056/NEJMoa043330

Sutter O, Calvo J, N'Kontchou G, Nault JC, Ourabia R, Nahon P, Ganne-Carrie N, Bourcier V, Zentar N, Bouhafs F, Sellier N, Diallo A, Seror O (2017) Safety and efficacy of irreversible electroporation for the treatment of hepatocellular carcinoma not amenable to thermal ablation techniques: a retrospective single-center case series. Radiology 284(3):877–886. https://doi.org/10.1148/radiol.2017161413

Swain SM, Im YH, Im SA, Chan V, Miles D, Knott A, Clark E, Ross G, Baselga J (2014) Safety profile of Pertuzumab with Trastuzumab and Docetaxel in patients from Asia with human epidermal growth factor receptor 2-positive metastatic breast cancer: results from the phase III trial CLEOPATRA. Oncologist 19(7):693–701. https://doi.org/10.1634/theoncologist.2014-0033

Tameez Ud Din A, Tameez-Ud-Din A, Chaudhary FMD, Chaudhary NA, Siddiqui KH (2019) Irreversible electroporation for liver tumors: a review of literature. Cureus 11(6):e4994. https://doi.org/10.7759/cureus.4994

Tamimi AF, Juweid M (2017) Epidemiology and outcome of glioblastoma. In: De Vleeschouwer S (ed) Glioblastoma. Codon Publications, Brisbane. https://doi.org/10.15586/codon.glioblastoma.2017.ch8

Thind K, Padrnos LJ, Ramanathan RK, Borad MJ (2017) Immunotherapy in pancreatic cancer treatment: a new frontier. Therap Adv Gastroenterol 10(1):168–194. https://doi.org/10.1177/1756283X16667909

Thomson KR, Cheung W, Ellis SJ, Federman D, Kavnoudias H, Loader-Oliver D, Roberts S, Evans P, Ball C, Haydon A (2011) Investigation of the safety of irreversible electroporation in humans. J Vasc Interv Radiol 22(5):611–621. https://doi.org/10.1016/j.jvir.2010.12.014

Usman M, Moore W, Talati R, Watkins K, Bilfinger TV (2012) Irreversible electroporation of lung neoplasm: a case series. Med Sci Monit 18(6):CS43–CS47. https://doi.org/10.12659/msm.882888

Vailas M, Syllaios A, Hashemaki N, Sotiropoulou M, Schizas D, Papalampros A, Felekouras E, Pikoulis E (2019) Irreversible electroporation and sarcomas: where do we stand? J BUON 24 (4):1354–1359

Valerio M, Stricker PD, Ahmed HU, Dickinson L, Ponsky L, Shnier R, Allen C, Emberton M (2014) Initial assessment of safety and clinical feasibility of irreversible electroporation in the focal treatment of prostate cancer. Prostate Cancer Prostatic Dis 17(4):343–347. https://doi.org/10.1038/pcan.2014.33

Valero V (1997) Docetaxel and cyclophosphamide in patients with advanced solid tumors. Oncology (Williston Park) 11(6 Suppl):21–23

van den Bos W, de Bruin DM, Jurhill RR, Savci-Heijink CD, Muller BG, Varkarakis IM, Skolarikos A, Zondervan PJ, Laguna-Pes MP, Wijkstra H, de Reijke TM, de la Rosette JJ (2016) The correlation between the electrode configuration and histopathology of irreversible electroporation ablations in prostate cancer patients. World J Urol 34(5):657–664. https://doi.org/10.1007/s00345-015-1661-x

Vizintin A, Vidmar J, Scancar J, Miklavcic D (2020) Effect of interphase and interpulse delay in high-frequency irreversible electroporation pulses on cell survival, membrane permeabilization and electrode material release. Bioelectrochemistry 134:107523. https://doi.org/10.1016/j.bioelechem.2020.107523

Vogel JA, van Veldhuisen E, Alles LK, Busch OR, Dijk F, van Gulik TM, Huijzer GM, Besselink MG, van Lienden KP, Verheij J (2019) Time-dependent impact of irreversible electroporation on pathology and ablation size in the porcine liver: a 24-hour experimental study. Technol Cancer Res Treat 18:1533033819876899. https://doi.org/10.1177/1533033819876899

Weaver JC, Chizmadzhev YA (1996) Theory of electroporation: a review. Bioelectrochem Bioenergetics 41(2):135–160

Wendler JJ, Fischbach K, Ricke J, Jurgens J, Fischbach F, Kollermann J, Porsch M, Baumunk D, Schostak M, Liehr UB, Pech M (2016) Irreversible Electroporation (IRE): standardization of terminology and reporting criteria for analysis and comparison. Pol J Radiol 81:54–64. https://doi.org/10.12659/PJR.896034

Wimmer T, Srimathveeravalli G, Gutta N, Ezell PC, Monette S, Kingham TP, Maybody M, Durack JC, Fong Y, Solomon SB (2013) Comparison of simulation-based treatment planning with imaging and pathology outcomes for percutaneous CT-guided irreversible electroporation of the porcine pancreas: a pilot study. J Vasc Interv Radiol 24(11):1709–1718. https://doi.org/10.1016/j.jvir.2013.05.056

Zeng J, Liu G, Li ZH, Yang Y, Fang G, Li RR, Xu KC, Niu L (2017) The safety and efficacy of irreversible electroporation for large hepatocellular carcinoma. Technol Cancer Res Treat 16 (1):120–124. https://doi.org/10.1177/1533034616676445

Zhang W, Wang W, Chai W, Luo X, Li J, Shi J, Bi L, Niu L (2017) Breast tissue ablation with irreversible electroporation in rabbits: a safety and feasibility study. PLoS One 12(7):e0181555. https://doi.org/10.1371/journal.pone.0181555

Zhao Y, Bhonsle S, Dong S, Lv Y, Liu H, Safaai-Jazi A, Davalos RV, Yao C (2018a) Characterization of conductivity changes during high-frequency irreversible electroporation for treatment planning. IEEE Trans Biomed Eng 65(8):1810–1819. https://doi.org/10.1109/TBME.2017.2778101

Zhao Y, Liu H, Bhonsle SP, Wang Y, Davalos RV, Yao C (2018b) Ablation outcome of irreversible electroporation on potato monitored by impedance spectrum under multi-electrode system. Biomed Eng Online 17(1):126. https://doi.org/10.1186/s12938-018-0562-9

Zhao J, Wen X, Tian L, Li T, Xu C, Wen X, Melancon MP, Gupta S, Shen B, Peng W, Li C (2019) Irreversible electroporation reverses resistance to immune checkpoint blockade in pancreatic cancer. Nat Commun 10(1):899. https://doi.org/10.1038/s41467-019-08782-1

Zupanic A, Kos B, Miklavcic D (2012) Treatment planning of electroporation-based medical interventions: electrochemotherapy, gene electrotransfer and irreversible electroporation. Phys Med Biol 57(17):5425–5440. https://doi.org/10.1088/0031-9155/57/17/5425